

9-2021

**IMPACT OF SODIUM DICHLOROACETATE ALONE AND IN  
COMBINATION THERAPIES ON LUNG TUMOR GROWTH AND  
METASTASIS**

Aya Mudhafar A. Al-Azawi

Follow this and additional works at: [https://scholarworks.uaeu.ac.ae/all\\_theses](https://scholarworks.uaeu.ac.ae/all_theses)



Part of the [Pharmacology Commons](#), and the [Toxicology Commons](#)

---

United Arab Emirates University  
College of Medicine and Health Sciences  
Department of Pharmacology and Therapeutics

IMPACT OF SODIUM DICHLOROACETATE ALONE AND IN  
COMBINATION THERAPIES ON LUNG TUMOR GROWTH AND  
METASTASIS

Aya Mudhafar A. Al-Azawi

This thesis is submitted in partial fulfilment of the requirements for the degree of  
Master of Medical Sciences (Pharmacology and Toxicology)

Under the Supervision of Professor Samir Attoub

September 2021

### Declaration of Original Work

I, Aya Mudhafar A. Al-Azawi, the undersigned, a graduate student at the United Arab Emirates University (UAEU), and the author of this thesis entitled “*Impact of Sodium Dichloroacetate Alone and in Combination Therapies on Lung Tumor Growth and Metastasis*”, hereby, solemnly declare that this thesis is my own original research work that has been done and prepared by me under the supervision of Professor Samir Attoub, in the College of Medicine and Health Sciences at UAEU. This work has not previously been presented or published or formed the basis for the award of any academic degree, diploma or a similar title at this or any other university. Any materials borrowed from other sources (whether published or unpublished) and relied upon or included in my thesis have been properly cited and acknowledged in accordance with appropriate academic conventions. I further declare that there is no potential conflict of interest with respect to the research, data collection, authorship, presentation and/or publication of this thesis.

Student's Signature:  \_\_\_\_\_ Date: 28/09/2021

Copyright © 2021 Aya Mudhafar A. Al-Azawi  
All Rights Reserved

## Approval of the Master Thesis

This Master Thesis is approved by the following Examining Committee Members:

- 1) Advisor (Committee Chair): Samir Attoub

Title: Professor

Department of Pharmacology and Therapeutics

College of Medicine and Health Sciences

Signature \_\_\_\_\_  \_\_\_\_\_ Date 28/09/2021

- 2) Member: Haider Raza

Title: Professor

Department of Biochemistry and Molecular Biology

College of Medicine and Health Sciences

Signature \_\_\_\_\_  \_\_\_\_\_ Date 28/09/2021

- 3) Member (External Examiner): Mohamed Rahmani

Title: Professor

Department of Molecular Biology and Genetics

Institution: Khalifa University, UAE

Signature \_\_\_\_\_  \_\_\_\_\_ Date 28/09/2021

This Master Thesis is accepted by:

Acting Dean of the College of Medicine and Health Sciences: Professor Juma Alkaabi

Signature  \_\_\_\_\_ Date 24/10/2021

Dean of the College of Graduate Studies: Professor Ali Al-Marzouqi

Signature  \_\_\_\_\_ Date 25/10/2021

Copy \_\_\_\_ of \_\_\_\_

## Abstract

Lung cancer is the second most common form of cancer with the highest mortality rate worldwide in 2020 despite the advances in targeted- and immuno-therapies. Metabolic reprogramming has been recognized as an essential emerging cancer hallmark in which altered metabolic pathways represent an attractive therapeutic target. Sodium Dichloroacetate (DCA), a pyruvate dehydrogenase kinase (PDK) inhibitor, effect has been investigated in various tumors. Building on the already published data, this pre-clinical study aims to explore the anticancer potential of DCA in lung cancer alone and in combination with chemo- and targeted therapies using two non-small cell lung cancer (NSCLC) cell lines namely, A549 and LNM35.

This project was addressed through the investigation of the impact of DCA on lung cancer cell viability, migration, invasion, and colony growth *in-vitro* and on tumor growth and metastasis using the chick embryo chorioallantoic membrane (CAM) and the nude mice models *in-vivo*. The anti-angiogenic potential of DCA, its safety profile, and the impact of its combination with the proposed chemotherapy and first-generation EGFR tyrosine kinase inhibitors (EGFR-TKi) were also investigated.

This study demonstrated that DCA causes a concentration- and time-dependent decrease in the viability of A549 and LNM35 cells and the growth of their colonies *in-vitro*. Similarly, DCA slow-down the growth of A549 and LNM35 tumor xenografts in both the chick embryo CAM and nude mice models *in-vivo*. DCA decreases the angiogenic capacity of human umbilical vein endothelial cells (HUVECs) *in-vitro* by decreasing HUVECs tube formation and sprouting, suggesting the inhibition of tumor angiogenesis as a potential mechanism behind its anti-tumor growth effect. On the other hand, DCA did not inhibit the *in-vitro* migration and invasion and the *in-vivo* incidence and growth of lymph nodes metastases in nude mice xenografted with the highly metastatic lung cancer cells LNM35. Treatment with DCA did not show any significant side effects on the chick embryos viability or on the nude mice weight and survival. In addition, blood, kidney, and liver function tests showed no toxicity with DCA when compared to the control group. Finally, DCA significantly enhanced the anticancer effect of cisplatin in LNM35, gefitinib and erlotinib in both cell lines.

In summary, these findings demonstrate that DCA is a safe and promising therapeutic agent for lung cancer and pave the way for further pre-clinical studies validating the impact of DCA in combination with not only the first generation but also the second and third generation of EGFR-Tki *in-vivo*.

**Keywords:** Lung cancer, Dichloroacetate, Pyruvate dehydrogenase kinase, Tumor growth, Angiogenesis, Chick embryo CAM.

## Title and Abstract (in Arabic)

### تأثير ثاني كلور أسيتات الصوديوم (Sodium Dichloroacetate) منفرداً أو مع العلاجات الأخرى على نمو و انتشار سرطان الرئة

#### المخلص

سرطان الرئة هو ثاني أكثر أنواع السرطانات انتشاراً مع أعلى معدل للوفيات في العالم خلال عام 2020، و هذا بالرغم من التقدم الهائل في العلاجات الإنتقائية (Targeted Therapy) و الأدوية المناعية (Immunotherapy). البرمجة الأيضية المعدلة (Metabolic Reprogramming) تعتبر هي إحدى مميزات مرض السرطان كسرطان الرئة حيث تعتبر المسارات الأيضية المعدلة في السرطان هدف مميز للعلاج. فاعلية ثاني كلور أسيتات الصوديوم (DCA)، مثبط إنزيم (PDK)، أختبرت في مختلف أنواع السرطان. بناءً على بعض الدراسات، تهدف هذه الدراسة إلى اختبار تأثير هذا الدواء على سرطان الرئة عندما يستخدم منفرداً أو منجماً مع العلاج الكيماوي (Chemotherapy) و العلاجات الإنتقائية (Targeted Therapy) و ذلك باستخدام نوعان من خلايا سرطان الرئة ذو الخلايا غير الصغيرة (A549) و (LNM35).

تضمنت هذه الدراسة اختبار مفعول هذا الدواء على قابلية الخلايا المذكورة على الحياة و النمو (Cellular viability)، نمو المستعمرات السرطانية (Colony growth)، هجرة و غزو الخلايا السرطانية (Migration) و (Invasion) إضافة إلى نمو الورم السرطاني في الفئران و على الغشاء المشيمي لفرخ الدجاجة (Chick Embryo Chorioallantoic Membrane). علاوة إلى ذلك، اختبار تأثير هذا الدواء على تكوين الأوعية الدموية (Angiogenesis)، سُميته و تأثيره على مفعول العلاج الكيماوي و الجيل الأول من الأدوية المثبطة لمستقبلات ال (EGF).

أظهرت هذه الدراسة قدرة ثاني كلور أسيتات الصوديوم (DCA) لتقليل قابلية خلايا سرطان الرئة للحياة و النمو و تكوين المستعمرات السرطانية مختبرياً و ذلك اعتماداً على تركيز و مدة العلاج. كما أظهرت فعالية الدواء في تقليل نمو الورم السرطاني في الفئران و الغشاء المشيمي لفرخ الدجاج و قد أظهرت الدراسة قدرة الدواء على منع تكوين الأوعية الدموية مختبرياً و التي قد تكون آلية مقترحة لعمل هذا الدواء في خلايا سرطان الرئة. في المقابل، لم يظهر الدواء فعالية في تقليل هجرة و غزو الخلايا السرطانية مختبرياً و انتشارها في الفئران. ثاني كلور أسيتات الصوديوم (DCA) لم يظهر أي تأثير سلبي على حياة فرخ الدجاجة أو الفئران و لم يظهر أي تأثير سلبي في صور الدم و وظائف الكبد و الكلى. و أخيراً، استخدام هذا الدواء مع بعض العلاجات المستخدمة لسرطان الرئة أظهرت قدرة ثاني كلور أسيتات الصوديوم (DCA) على تحسين فاعلية دواء (Cisplatin) ضد أحد الأنواع المستخدمة من خلايا سرطان الرئة و المعروفة باسم سرطان الخلايا الكبيرة – (Large Cell Carcinoma – LNM35)، و الأدوية الإنتقائية (Erlotinib) و (Gefitinib) في كلا النوعين من الخلايا المستخدمة.

هذه الدراسة أثبتت أمان و فاعلية ثاني كلور أسيتات الصوديوم (DCA) ضد سرطان الرئة عندما يستخدم وحيداً أو مع بعض الأدوية المثبتية و بهذا تعتبر هذه الدراسة تمهيد لدراسات مستقبلية للتحقق من تأثير ثاني كلور أسيتات

الصوديوم (DCA) على مفعول الجيل الأول من الأدوية الإنتقائية المثبطة لمستقبلات ال (EGF) في جسم الكائن الحي إضافة إلى الجيل الثاني و الثالث من هذه الأدوية الإنتقائية المثبطة.

**مفاهيم البحث الرئيسية:** سرطان الرئة، ثاني كلور أسيتات الصوديوم، pyruvate dehydrogenase kinase، نمو الورم، تكوين الأوعية الدموية، الغشاء المشيمي لفرخ الدجاجة.

## Acknowledgements

First and foremost, praises and thanks to the almighty God for paving the way to join this journey and for all the blessings granted to finish this work.

It is my pleasure to express my deep sense of thanks and appreciation to my supervisor and mentor Prof. Samir Attoub, for joining his team and guiding me throughout my study and research. His valuable assistance, unique scientific approach, fruitful discussions, patience and dedication to always do better have widened my horizon and helped me to improve my research skills, writing skills and scientific thinking.

I would like to extend my gratitude to the best lab members and second family, Mrs. Kholoud and Shahrazad for their time and endless cooperation. Their support and care create an enjoyable environment to work and achieve.

I thank profusely the UAE university for giving me the chance to join the college of Medicine and Health Sciences and for providing me with all the necessary materials, instruments and services to study and do research. It is my pleasure to be one of the university graduates.

I'm extremely grateful to my parents for their believing in me starting when I was young and till now. I'm sure I will not be here today without their endless love, unlimited sacrifice, various support and encouragement. I will always be blessed and grateful for having them in my life. I also owe a deep sense of gratitude to my uncle Dr. Adnan Al-Azawi, my aunts Selma, Ibtisam and Khawla and my friends Shifaa and Menna for their continuous support as well as my fiancé Rabei for his inspiration,

valuable advice tips and confidence.

Finally, my gratitude and appreciation are extended to the ones who first introduced me to the research in cancer field, Prof. Raafat El-Awady, Professor of Pharmacology at Sharjah University and Prof. Ekram Salih, Professor of Biochemistry. Their enthusiasm, values, unique advice and efforts have established the foundation stone for my career years ago.

## **Dedication**

*To my beloved parents and family*

## Table of Contents

Title .....	i
Declaration of Original Work .....	ii
Copyright .....	ii
Approval of the Master Thesis .....	iv
Abstract .....	vi
Title and Abstract (in Arabic) .....	viii
Acknowledgements .....	x
Dedication .....	xii
Table of Contents .....	xiii
List of Tables.....	xv
List of Figures .....	xvii
List of Abbreviations.....	xviii
Chapter 1: Introduction .....	1
1.1 Lung Cancer Risk Factors .....	2
1.2 Lung Cancer Types .....	3
1.3 Lung Cancer Stages.....	3
1.4 NSCLC Treatment.....	5
1.5 Cancer Hallmarks .....	6
1.5.1 Angiogenesis in Cancer.....	6
1.5.2 Invasion & Metastasis in Cancer.....	9
1.5.3 Metabolic Reprogramming .....	13
1.6 Dichloroacetate (DCA) .....	15
1.7 Aim and Objectives .....	16
Chapter 2: Materials and Methods .....	18
2.1 Cell Culture and Reagents.....	18
2.2 Cellular Viability.....	18
2.3 Clonogenic Assay .....	20
2.4 <i>In Ovo</i> Tumor Growth Assay .....	20
2.6 Vascular Tube Formation Assay .....	25
2.7 HUVEC Spheroids Sprouting Assay .....	25
2.8 Wound Healing Motility Assay .....	27
2.9 Matrigel Invasion Assay .....	27
2.10 Statistical Analysis .....	28
Chapter 3: Results .....	30

3.1 Effect of DCA on Cellular Viability and Colony Growth of NSCLC Cell Lines .....	30
3.2 Effect of DCA on the Growth of NSCLC Tumor Xenografts in the Chick Embryo CAM and Nude Mice <i>In-Vivo</i> .....	32
3.3 Effect of DCA on the Formation of Capillary-Like Structures and Sprouting by HUVECs <i>In-Vitro</i> .....	37
3.4 Effect of DCA on NSCLC Metastasis <i>In-Vivo</i> and Invasion and Migration <i>In-Vitro</i> .....	40
3.5 Effect of DCA in Combination with Chemotherapeutic Agents on the Viability of NSCLC Cells.....	43
3.6 Effect of DCA in Combination with Frondoside A on NSCLC Cellular Viability and Colony Growth.....	45
3.7 Effect of DCA in Combination with EGFR-TKi on NSCLC Cellular Viability and Colony Growth.....	47
Chapter 4: Discussion .....	51
Chapter 5: Conclusion.....	61
References .....	62

**List of Tables**

Table 1: Treatment Options of NSCLC .....5

## List of Figures

Figure 1: Angiogenic Process in Cancer .....	8
Figure 2: Invasion-Metastasis Cascade .....	10
Figure 3: Biochemical Steps of Aerobic Glycolysis .....	15
Figure 4: Schematic Representation for the Detection of Viable cells using CellTiter-Glo® Luminescent Cell Viability Assay .....	19
Figure 5: Schematic Representation of the <i>In-Ovo</i> Tumor Growth Assay .....	22
Figure 6: Schematic Representation of Xenografting A549 Cells into the Nude Mice and the Oral Treatment with DCA 50 mg/kg and 200 mg/kg .....	24
Figure 7: Schematic Representation of Xenografting LNM35 Cells into the Nude Mice and the Oral Treatment with DCA 200 mg/kg and 500 mg/kg .....	24
Figure 8: Preparation of Hanging Drops for Spheroid Preparation .....	26
Figure 9: Schematic Representation of the Invasion Chamber Assay .....	28
Figure 10: Effect of DCA on NSCLC Cells Viability and Colony Growth.....	31
Figure 11: Effect of DCA on the Growth of A549 and LNM35 Tumor Xenografts in the Chick Embryo Chorioallantoic Membrane (CAM) <i>In-Vivo</i> .....	32
Figure 12: Effect of DCA on the Growth of A549 Xenografted in Nude Mice <i>In-Vivo</i> .....	34
Figure 13: Effect of DCA on the Growth of LNM35 Xenografted in Nude Mice <i>In-Vivo</i> .....	36
Figure 14: Effect of DCA on the Formation of Capillary-Like Structures by HUVECs <i>In-Vitro</i> .....	38
Figure 15: Effect of DCA on the Formation of Sprouts by the Embedded HUVECs Spheroids <i>In-Vitro</i> .....	39
Figure 16: Effect of DCA on NSCLC Metastasis <i>In-Vivo</i> .....	40
Figure 17: Effect of DCA on NSCLC cells Migration and Invasion <i>In-Vitro</i> .....	41
Figure 18: Effect of DCA in Combination with Chemotherapeutic Agents on the Viability of NSCLC Cells.....	44
Figure 19: Effect of DCA in Combination with Frondoside A on NSCLC Cells Viability and Colony Growth.....	46
Figure 20: Effect of EGFR-Tki on NSCLC Cells Viability.....	48
Figure 21: Effect of DCA in Combination with Gefitinib on NSCLC Cells Viability and Colonies .....	49

Figure 22: Effect of DCA in Combination with Erlotinib on  
NSCLC Cells Viability and Colonies ..... 50

## List of Abbreviations

ADC	Adenocarcinoma
AMPK	AMP-activated Protein Kinase
CAM	Chorioallantoic Membrane
COPD	Chronic Obstructive Pulmonary Disease
CRC	Colorectal Cancer
CTCs	Circulating Tumor Cells
DCA	Dichloroacetate
ECM	Extracellular Matrix
EGFR-TKi	Epidermal Growth Factor Receptor Tyrosine Kinase inhibitors
EMT	Epithelial-Mesenchymal Transition
FGF	Fibroblast Growth Factor
GLUT1	Glucose Transporter 1
HIF-1	Hypoxia-inducible Factor-1
ICAM-1	Intercellular Adhesion Molecule-1
LCC	Large Cell Carcinoma
LDHA	Lactate Dehydrogenase A
MCT4	Monocarboxylate Transporter 4
MMPs	Matrix Metalloproteinases
mtDNA	Mitochondrial DNA
MTP	Mitochondrial Transition Pores
NSCLC	Non-Small Cell Lung Cancer
OXPHOS	Oxidative Phosphorylation

PAH	Polycyclic Aromatic Hydrocarbons
PDGF	Platelet-Derived Growth Factor
PDH	Pyruvate Dehydrogenase
PDK	Pyruvate Dehydrogenase Kinase
PIGF	Placental Growth Factor
PKM2	Pyruvate Kinase M2
SCC	Squamous Cell Carcinoma
SCLC	Small Cell Lung Cancer
TAMs	Tumor Associated Macrophages
TME	Tumor Microenvironment
TSNAs	Tobacco-Specific N-nitrosamine
VCAM-1	Vascular Cell Adhesion Molecule-1
VEGF	Vascular Endothelial Growth Factors

## **Chapter 1: Introduction**

Cancer is a multifactorial disease characterized by abnormally divided cells due to some genetic or epigenetic changes that disrupt the cellular mechanisms controlling proliferation, survival and differentiation (Katzung et al., 2012; Malarkey et al., 2013). These transformed cells can disrupt the collaborative integration of the human body causing negative consequences on health, quality of life and survival of the human being (El-Metwally, 2009). Cancer can be classified according to the primary site, the first site in the body where cancer starts developing or by the tissue type in which the cancer arises into carcinoma, sarcoma, leukemia, lymphoma and myeloma (National Cancer Institute, 2020). Carcinoma is the most common type of cancer and it resembles all the malignancies of the epithelial tissues that form the internal and external lining of the body while sarcoma represents the cancer of connective or soft tissues such as bones and muscles (El-Metwally, 2009). Leukemia, lymphoma and myeloma refer to the malignancies of blood-forming tissue of the bone marrow, lymphocytes and plasma cells, respectively (National Cancer Institute, 2020).

In 2020, there were globally 19 million new cancer cases and 10 million deaths which make cancer as the second leading cause of death after cardiovascular diseases worldwide (WHO, 2020). 12% of these new cancer cases and 18% of the deaths account for the lung cancer to be the second most commonly occurring cancer after breast cancer and a leading cause of cancer mortality among all other types worldwide in 2020. It is predicted that lung cancer incidence and mortality will continue to raise in the next twenty years by approximately 60% to reach 3.6 million new cases and 3 million deaths in 2040 (IARC-WHO, 2020). The continuous growing of this global

burden along with the associated morbidity, mortality, cost and therapy limitations have motivated further research to investigate the biology of lung cancers and develop novel therapeutic approaches for better outcomes of the disease.

### **1.1 Lung Cancer Risk Factors**

Factors, that may contribute to the development of lung cancer, can be classified into behavioral, environmental, biological and genetic factors (de Groot et al., 2018). Firstly, behavioral factors include tobacco smoking which is considered as the major risk factor since it is responsible for up to 90% of lung cancer cases (de Groot et al., 2018). Tobacco composition has been linked to its carcinogenic effects. Nicotine, a major constituent of tobacco, is responsible for the tobacco dependence and progression of already developed lung cancer (Costa & Soares, 2009; de Groot et al., 2018). Additionally, 60 other substances, such as: polycyclic aromatic hydrocarbons (PAH), nitrates and tobacco-specific N-nitrosamine (TSNAs), were identified from tobacco combustion and were classified as carcinogens that cause DNA adducts and free radical damage (Hecht, 2012). Secondly, environmental risk factors include air pollution and occupational exposure to carcinogens, such as: radon, asbestos, arsenic, cadmium, nickel and silica (Dela Cruz et al., 2011). On the other hand, Chronic obstructive pulmonary disease (COPD), that is characterized by chronic airway inflammation and airflow obstruction, pulmonary fibrosis of different etiologies (Parker et al., 2017) and infection diseases with viruses such as: HPV, Epstein-Barr virus, chlamydia pneumonia and HIV (Dela Cruz et al., 2011) have been associated with an increased risk of developing lung cancer in smokers and non-smokers. Genetic abnormalities have been studied extensively and linked to increased risk of lung cancer development. These abnormalities can be inherited or acquired

during individual's lifetime increasing the susceptibility to lung cancer (de Groot et al., 2018).

## **1.2 Lung Cancer Types**

Lung cancer originates from the respiratory cells of epithelial origin. It has been classified histologically into Non-small cell lung cancer (NSCLC) which is considered as the most common type with 80-85% of all lung cancer cases and Small cell lung cancer (SCLC) accounts for 10-15% of all lung cancer cases (American Cancer Society, 2016; Dela Cruz et al., 2011). NSCLC has been further classified into Adenocarcinoma (ADC), Squamous cell carcinoma (SCC) and large cell carcinoma (LCC) that are similar in the treatment approaches and prognosis but different in the clinical characteristics and the cells type from which the cancer arises (American Cancer Society, 2016; Tan & Huq, 2021). Adenocarcinoma originates from the alveolar surface epithelium or the mucosal glands in the bronchi while squamous cell carcinoma arises from the proximal segmental bronchi. The latter subtype is slowly growing which can take years to be a clinically evident tumor. Large cell carcinoma can originate in any part of the lungs with rapidly growing and spreading capacity (Houlihan & Tyson, 2012). On the other hand, SCLC is a neuroendocrine tumor that grows and spreads faster than NSCLC (National Cancer Institute, 2018).

## **1.3 Lung Cancer Stages**

Staging is the process of determining the extent of cancer in order to determine the prognosis and the most appropriate treatment plan with subsequent evaluation for the treatment response. Regarding lung cancer, the international TNM-based staging system has been used commonly in which T represents the extent and size of the

primary tumor, N indicates the extent of affected nearby lymph nodes and M indicates the presence or absence of metastasis. Each category is followed by a value resembling the extent of cancer. The different combinations of TNM values can be grouped into stages range from I to IV in NSCLC and Limited or Extensive stage in SCLC. The lower the stage number, the less advanced cancer is, and better prognosis in comparison to the higher stage number (Lemjabbar-Alaoui et al., 2015).

In-situ NSCLC resembles stage 0 that is characterized by the development of cancer in a specific place without any spread beyond that. Early-stage NSCLC includes stage I, with the substages IA and IB, and stage II, with substages IIA and IIB. Stage I is characterized by the presence of small primary tumor in one lung with size range 0-4cm without any spread to lymph nodes or distant places. Stage II (IIA, IIB) is characterized by non-metastasizing primary tumor ranging between 4-7cm in size that has or has not spread to lymph nodes. Locally advanced NSCLC stage is the stage III (IIIA, IIIB, IIIC) in which the cancer has spread within the chest but not metastasized to distant parts of the body with or without involvement of the lymph nodes. Finally, stage IV (IVA, IVB) NSCLC is known as metastatic NSCLC stage in which the tumor is of any size that has metastasized to one or multiple sites outside the chest and may or may not spread to lymph nodes (Amin et al., 2017; Detterbeck, 2018).

In SCLC, limited stage resembles the presence of tumor in one lung with or without the involvement of nearby lymph nodes. On the other hand, extensive stage resembles the spread of cancer into both lungs or distant organs and lymph nodes (American Cancer Society, 2019).

## 1.4 NSCLC Treatment

Significant advances have been made in the management of NSCLC by the addition of various classes of targeted and immunotherapy to the chemotherapy (Table 1). Single or combined approach of surgery, radiotherapy, chemotherapy, targeted and immunotherapy is followed depending on the stage, histology, genetic alterations and patient's condition (Alexander et al., 2020).

Table 1: Treatment Options of NSCLC.

Treatment	Major Class	
Chemotherapy	Alkylating agents	▪ Cisplatin, Carboplatin
	Plant Derivatives	▪ Paclitaxel, Docetaxel ▪ Vinorelbine ▪ Etoposide
	Antimetabolites	▪ Gemcitabine ▪ Pemetrexed
Targeted therapy	Angiogenesis inhibitors	▪ Bevacizumab ▪ Ramucirumab ▪ Aflibercept ▪ Nintedanib, Axitinib, Sorafenib, Afatinib, Anlotinib
	EGFR inhibitors	▪ Erlotinib, Gefitinib, Afatinib, Osimertinib, Dacomitinib
	ALK inhibitors	▪ Crizotinib, Ceritinib, Alectinib, Brigatinib, Lorlatinib
	ROS1 inhibitors	▪ Crizotinib, Ceritinib, Lorlatinib, Entrectinib
	BRAF/MEK inhibitors	▪ Dabrafenib ▪ Trametinib
	RET Inhibitors	▪ Selpercatinib, pralsetinib
	MET inhibitors	▪ Capmatinib, tepotinib
	Immunotherapy	PD-1/PD-L1 inhibitors
CTLA-4 inhibitors		▪ Ipilimumab

Surgery is considered as the mainstay treatment in medically fit patients with NSCLC staging I through IIIA. Radiotherapy is an option for patients with unresectable tumor and it can play a crucial part in palliative care to improve the patient's quality of life. Chemotherapy is indicated in some neoadjuvant and adjuvant

settings in addition to advanced NSCLC. Targeted therapy can be applied in patients with advanced stage having genetic alterations of EGFR, ALK, ROS1, RET, BRAF V600E, MET Exon 14, and NTRK. Additionally, Immunotherapy has been indicated alone or in combinational therapies in advanced NSCLC (Alexander et al., 2020; Zappa & Mousa, 2016).

## **1.5 Cancer Hallmarks**

The complex cellular capabilities acquired during the multistage process of carcinogenesis has been organized in a conceptual framework of cancer hallmarks to facilitate the understanding of cancer biology. Cancer hallmarks involve the acquired advantageous characteristics that promote the transformation of normal cells and the subsequent progression of the malignant cells while exploiting the host tissue (Fouad & Aanei, 2017). Cancer hallmarks include: sustaining proliferative signaling, evading growth suppressors, resisting cell death, enabling replicative immortality, inducing angiogenesis, activating invasion and metastasis, metabolic rewiring and evading immune destruction (Alkhazraji et al., 2019).

### **1.5.1 Angiogenesis in Cancer**

Angiogenesis is a process of forming new blood vessels from pre-existing vasculature in contrast to vasculogenesis that resembles the de novo formation of blood vessels as a consequence of the differentiation of vascular progenitor cells (Zuazo-Gaztelu & Casanovas, 2018). Angiogenesis implies in different physiological conditions such as: embryogenesis, wound healing, and menstrual cycle in which the process is highly regulated by multiple stimulatory and inhibitory growth factors (Saman et al., 2020). Stimulatory growth factors include Vascular Endothelial Growth

Factor (VEGF), Fibroblast Growth Factor (FGF), Transforming Growth Factors alpha and beta, Interleukin-8 and Granulocyte Colony-Stimulating Factor. On the other hand, inhibitory growth factors include Angiostatin, Endostatin, Interferons, retinoids and Interleukin-12 (Carmeliet, 2003). Additionally, specific microRNA, known as angiomiRs, have been studied extensively for their crucial role in regulating the process of angiogenesis (Wang & Olson, 2009).

Angiogenesis has also been involved in unregulated manner in various pathological conditions including cancer. Involvement of angiogenesis in malignant conditions is considered as one of the hallmarks that promote progression and metastasis of several tumors, including NSCLC (Manzo et al., 2017; Tonini et al., 2003). In order for the tumor to grow further in size, sufficient oxygen, nutrients, and metabolic waste elimination need to be provided by adequate vasculature which can also be an access for tumor cells to metastasize into distal parts of the body (Nishida et al., 2006). The angiogenic switch starts with activating the transcription of multiple genes encoding the angiogenic molecules such as: PDGF, VEGF and FGF (Zuazo-Gaztelu & Casanovas, 2018). VEGF family includes VEGF-A, VEGF-B, VEGF-C, VEGF-D, VEGF-E and placental growth factor (PlGF). VEGF-A is a particularly essential angiogenic activator that is produced by tumor cells and the different types of cells present in the tumor microenvironment, including infiltrating macrophages, mast cells, neutrophils, platelets, stromal fibroblasts and endothelial cells (Hall & Ran, 2010). It is expressed due to different stimuli such as: hypoxia, hypoglycemia, overexpression of the oncogene Myc (Mezquita et al., 2005), downregulation of tumor suppressor genes (Fernando et al., 2008) and lactate accumulation in tumor microenvironment (Shi et al., 2001).

As shown in Figure 1, the angiogenic switch, triggered by the VEGF binding to its receptor, will be followed by destabilization of the endothelial-pericyte contacts that maintain the stability of the quiescent vessels (Zuazo-Gaztelu & Casanovas, 2018). During the sprouting process, VEGF signals will cause part of the endothelial cells, known as tip cells, to extend large filopodia to guide the newly formed vessel in addition to secreting some signals to recruit stromal cells for vessel stabilization. Another part of endothelial cells, that are located at the stalk of the angiogenic sprout, evolve into highly proliferative cells that will be responsible for the tube and branch formation (Gerhardt et al., 2003). Stalk cells also collaborate in the basement membrane deposition and establish junctions with adjacent cells to strengthen the new sprout (Dejana et al., 2009). At the end, tip cells interconnect in vessel loops that will turn off their leading function, suppress the angiogenic signals and decrease the VEGF levels to reestablish the quiescence. The stabilization and maturity of newly formed vessels will be achieved by forming new basement membrane and recruiting pericytes (Zuazo-Gaztelu & Casanovas, 2018).

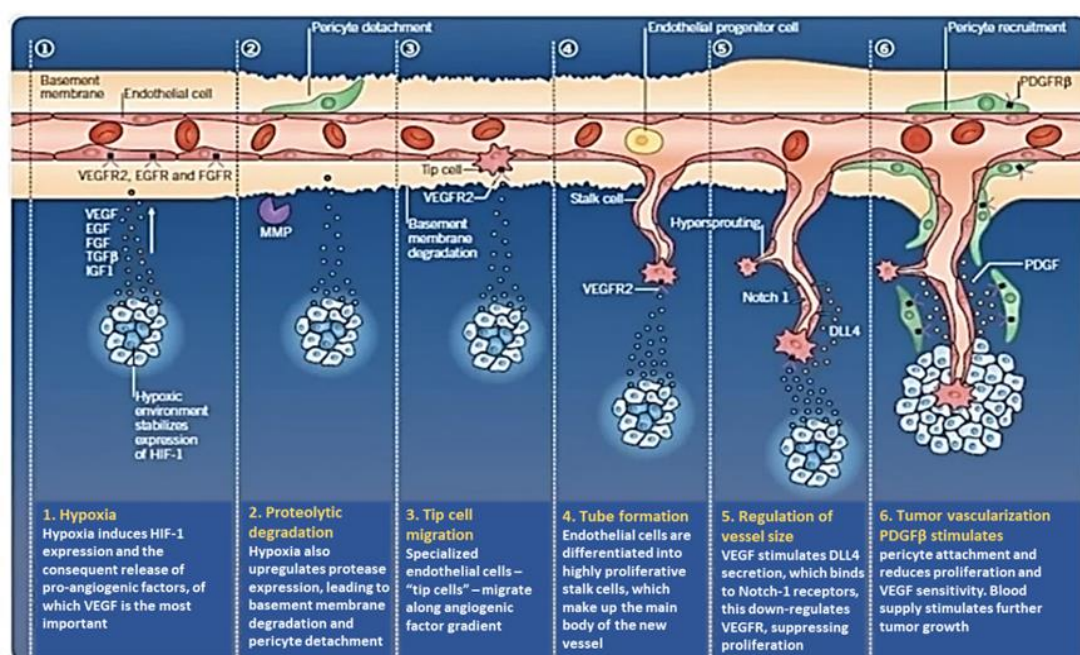


Figure 1: Angiogenic Process in Cancer (Tocris Bioscience, 2019).

The unregulated angiogenic process, due to sustained angiogenic signals in the tumor microenvironment (TME), results in abnormal excessive tumor vessels that are immature, dilated and hyperpermeable due to the irregular endothelial monolayers and abnormal coverage by the pericyte and basement membrane (Hapach et al., 2019; Hida et al., 2016). This nature of tumor vessels results in chaotic and uneven blood flow within the tumor resulting in persistent or intermittent hypoxia and acidosis in some parts within the tumor that can contribute to efficacy reduction in cancer therapy and development of resistance to cancer therapy (Lugano et al., 2020). Hence, anti-angiogenic therapy has been approved to be an effective strategy in the combinational treatment of several cancers including NSCLC (Tian et al., 2020). VEGF-A antibody, Bevacizumab, has been approved to use with platinum-based chemotherapy as a first-line treatment of patients with advanced non-squamous NSCLC. Additionally, Ramucirumab and Nintedanib are used in combination with docetaxel as a second-line treatment of patients with non-squamous NSCLC or any histology, respectively (Janning & Loges, 2018; Manzo et al., 2017). Despite of the major advances in the development of angiogenesis inhibitors, efficacy is modest in most tumors due to the high tendency for resistance, increased local invasion and distant metastasis (Ribatti et al., 2019) in addition to serious side effects, such as bleeding and hypertension. Therefore, intensive research efforts are being engaged to develop more efficacious and safe agents (Tian et al., 2020).

### **1.5.2 Invasion & Metastasis**

At the time of diagnosis, approximately 30-40% of NSCLC patients are diagnosed with metastatic stage to common sites, including bone, lungs, brain, adrenal glands and liver (Tamura et al., 2015). Poor prognosis and low survival rates are still

accompanying the patients with metastatic lung cancer despite of the recent revolution in targeted and immune therapy (Lu et al., 2019). Therefore, several new therapeutic agents are being investigated in the clinical settings to enrich the treatment options for patients with advanced disease to improve their survival and quality of life.

Cancer is characterized by its ability to invade the adjacent tissues and metastasize to distal organs forming secondary growths (Fouad & Aanei, 2017). It has been reported that metastasis is a leading cause of cancer-related mortality (Meirson et al., 2020). As shown in Figure 2, cancer invasion and metastasis occur through series of events known as invasion-metastasis cascade that involve invasion and migration through the extracellular matrix (ECM), intravasation into vasculature or lymphatic system, surviving transportation through circulation, extravasation into distal organs and formation of micro- and macrometastases (Fouad & Aanei, 2017; Hapach et al., 2019).

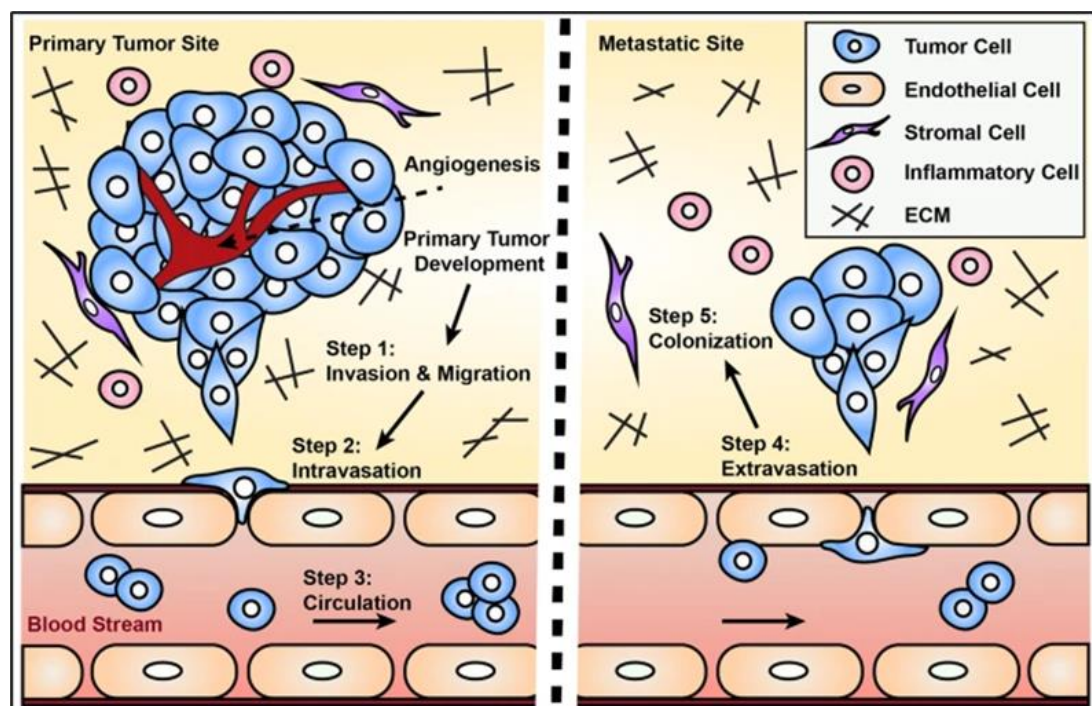


Figure 2: Invasion-Metastasis Cascade (Hapach et al., 2019).

Detachment, invasion, and motility of various cancer cells were linked to epithelial-mesenchymal transition (EMT), amoeboid transcription or collective migration (Perlikos et al., 2013). EMT is characterized by the loss of immobile and tightly adherent characteristics of the epithelial cells and gaining the motile characteristics of mesenchymal cells (Kalluri & Weinberg, 2009). One of the EMT hallmarks is downregulating or losing the E-cadherin by different transcriptional suppressors, such as: Snail/SNAI1, Slug/SNAI2, SIP1/ZEB2 or Twist. E-cadherin is an essential component of adherence junctions between the epithelial cells. It binds extracellularly to an E-cadherin molecule of the adjacent epithelial cell to stabilize the intercellular connections and links intracellularly to  $\beta$ -catenin,  $\alpha$ -catenin and p120-catenin to connect the junctions to the cytoskeleton and control some intracellular signaling. E-cadherin downregulation cause demounting of the adherence junctions and translocation of the  $\beta$ -catenin to the nucleus where it modulates transcription of numerous genes such as c-myc or cyclin D1 (Harris & Tepass, 2010; Van Zijl et al., 2011). Another hallmark of ENT is the upregulation of vimentin and neuronal (N-)cadherin that will activate Rac1 and Cdc42 which will in turn mediate the Rho-induced stress fibers and the formation of lamellipodia and filopodia, respectively (Yamao et al., 2015). Hence, cells that have undergone EMT, including the cadherin-switch from E- to N-cadherin expression, loose their organization and detach from the cell clusters to move through the ECM (Harris & Tepass, 2010). Motility and invasion via EMT process requires matrix metalloproteinases (MMPs) to degrade the ECM (Fouad & Aanei, 2017; Perlikos et al., 2013). MMPs have been found to be highly expressed in various types of cancer and the expression of some members become a sign for poor prognosis (Hadler-Olsen et al., 2013). On the contrary, cancer cells

moving via amoeboid motion will take the spherical morphology and slip through pre-existing channels in the ECM without the need of producing or activating MMPs. In addition to the EMT and amoeboid motion, the third type of cancer cell motility is the collective migration in which clusters of cells move together with the presence of adhesion proteins (Perlikos et al., 2013).

Intravasation is the process by which the invasive cells get into the vasculature lumen (Chiang et al., 2016). It starts with the attraction of tumor cells toward the blood vessels because of the EGF secreted by the tumor associated macrophages (TAMs) that are accumulated along the blood vessels and tumor margins. Additionally, lymphatic endothelial cells secrete CCL21 or CXCL12 to enable the chemotaxis of the tumor cells expressing CCR7 or CXCR4 receptors (Perlikos et al., 2013). Intravasation can be induced by different chemical and physical signals provided by the tumor microenvironment. For instance, stiffened ECM promote intravasation by increasing the vascular permeability (Wang et al., 2019). Intravasation occurs by passive entry through the gaps in the endothelial wall or by lining the blood vessels and replacing the endothelial cell creating a mosaic model (Perlikos et al., 2013). Upon reaching the circulation, circulating tumor cells (CTCs) will survive the harsh conditions, such as: hemodynamic shear forces, immune stresses, and red blood cell collisions by two mechanisms depending on the cell type. Physical collision occurs when the CTCs stuck in the vessel because of their larger diameter compared to the vessel traveling through. On the other hand, rolling-adhesion occurs upon collision of CTCs with the endothelium followed by rolling via E-selectin or P-selectin binding and arrest via binding with intercellular adhesion molecule-1 (ICAM-1) or vascular cell adhesion molecule-1 (VCAM-1) (Hapach et al., 2019). Another mechanism was suggested to

survive the stressful conditions in the circulation is the formation of microemboli with thrombocytes and erythrocytes (Perlikos et al., 2013). The CTCs will extravasate and arrest to secondary sites following the mechanical arrest mechanism or the selective arrest mechanism. Mechanical arrest occurs in organ where there are dense of capillaries such as: lungs, liver, brain and bone while selective arrest mechanism occurs at specific organs. The latter mechanism can be explained by the endothelial adhesion molecules that are different between the organ vessels. For instance, breast cancer cells expressing the CXCR4 receptors are commonly extravasate to the liver, lung, bone marrow and lymph nodes because of the expression of CXCL12 ligand on their vessels (Perlikos et al., 2013). After extravasation, the majority of surviving cells will be dormant and small percentage will continue growing to form new tumor. The dormancy of the surviving cells can be due to the cytotoxic effect of the immune cells or the lack of sufficient blood supply. The mechanism behind the escape of the dormant cells to the colonization step is poorly understood (Fouad & Aanei, 2017).

### **1.5.3 Metabolic Reprogramming**

Cellular metabolism involves network of biochemical reactions to produce energy and macromolecules in order to meet tissue demands for homeostasis, growth and maintaining cellular functions (Faubert et al., 2020). Normal cells utilize the cytosolic glycolysis followed by the mitochondrial oxidative phosphorylation (OXPHOS) to produce energy in the presence of oxygen. Under anerobic conditions, normal cells rely mainly on the cytosolic glycolysis to produce energy. It has been found that cancer cells deviate from such normal metabolic phenotype by relying mainly on glycolysis even in the presence of oxygen. This phenomenon was termed as Warburg Effect relating to the German Scientist Otto Warburg (Yoshida, 2015). This

metabolic shift has been considered as a hallmark of cancer which is acquired during the early stages of carcinogenesis to support cancer proliferation and progression (Vaupel & Multhoff, 2021). Alteration of metabolism in tumor tissues results from variety of factors including: normoxic/hypoxic activation of the transcription factor hypoxia-inducible factor-1 (HIF-1), activation of oncogenes, inactivation of tumor suppressors and alteration of various signaling pathways such as: PI3K–Akt–mTORC1 signaling pathway and AMP-activated protein kinase (AMPK) signaling pathway. In addition to that, Warburg effect can be caused by mitochondrial dysfunctions due to mutations in the mitochondrial DNA (mtDNA) or in the genes encoding the Krebs cycle enzymes (Vaupel et al., 2019).

Aerobic glycolysis involves a multi-step cytosolic catabolism of glucose to pyruvate followed by conversion to lactate which is exported to the extracellular space. As shown in Figure 3, several transcriptional activations have been noted in this pathway such as: Glucose transporter (GLUT1), monocarboxylate transporter 4 (MCT4) for exporting lactate, and key glycolytic enzymes: hexokinase 2, phosphofructokinase 1, enolase 1, pyruvate kinase M2 (PKM2), lactate dehydrogenase A (LDHA) and the mitochondrial pyruvate dehydrogenase kinase (PDK) (Vaupel & Multhoff, 2021). The latter enzyme comprises of four isozymes (PDK1-4) that are located in the mitochondrial matrix. PDKs indirectly inhibit the oxidative conversion of pyruvate to acetyl-CoA in the mitochondria by phosphorylating Ser293, Ser300, and Ser232 of E1 $\alpha$  subunit of the gatekeeper enzyme pyruvate dehydrogenase (PDH). Inhibition of PDH will push the pyruvate away from the mitochondria and be converted to lactate in the cytosol (Woolbright et al., 2019). Expression of PDKs is altered in a variety of cancers. Upregulation of PDKs in cancer can be due to various

transcription factors including HIF1 $\alpha$ . Hypoxia and/or genetic mutations in Akt and mTOR signaling pathways during normoxia can stabilize and translocate HIF1 $\alpha$  to the nucleus to upregulate multiple genes involved in glycolysis, including PDKs (Levine & Puzio-Kuter, 2010; Semenza, 2013). Therefore, PDKs have been widely studied as a potential therapeutic target for cancer treatment (Stacpoole, 2017).

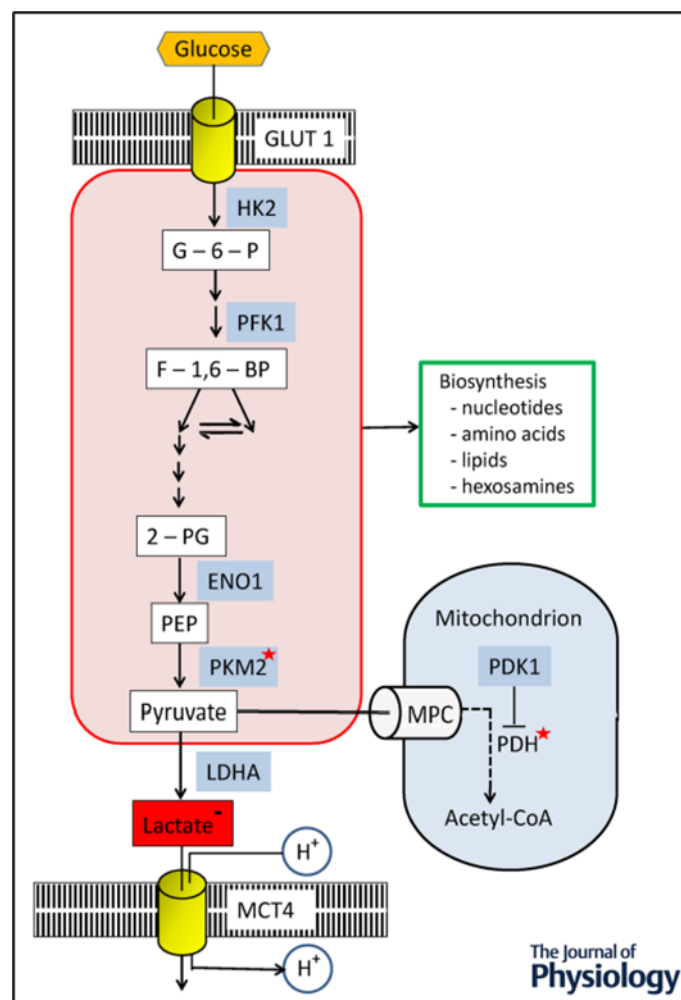


Figure 3: Biochemical Steps of Aerobic Glycolysis (Vaupel and Multhoff, 2021).

### 1.6 Dichloroacetate (DCA)

DCA is a salt of Dichloroacetic acid that is characterized by its small molecular weight and water solubility explaining the high drug bioavailability. It is an analog of

acetic acid in which two hydrogen atoms of the methyl group are replaced by chlorine atoms (Tataranni & Piccoli, 2019). In the last decade, DCA was used in lactic acidosis, congenital disease of mitochondrial metabolism and diabetes mellitus. The potential role of DCA in the management of cancer is due to its ability to reverse the Warburg effect (James et al., 2017). DCA inhibits the four isoenzymes of Pyruvate Dehydrogenase Kinase (PDK) with favorable inhibition of isoenzyme II, an enzyme that phosphorylates and deactivates the Pyruvate Dehydrogenase (PDH). Upon inhibition of PDK by DCA, the mitochondrial-dependent glucose oxidation will be promoted due to the increase in the PDH activity and the influx of pyruvate into the mitochondria (Kankotia & Stacpoole, 2014). Consequently, mitochondrial transition pores (MTP) will be opened and allow for the pro-apoptotic mediators to be released from the mitochondria to the cytoplasm resulting in the apoptotic cascade which will be selective for the cancer cells (Michelakis et al., 2008). It has been found that DCA possess anti-tumor activities *in-vitro* in NSCLC (Bonnet et al., 2007), head and neck squamous cell carcinoma models (Sun et al., 2009), colorectal (Madhok et al., 2010), breast (Sun et al., 2010), T-cell lymphoma (Kumar et al., 2012).

### **1.7 Aim and Objectives**

While the global burden of lung cancer is continuously growing, targeting metabolic reprogramming has become an attractive approach to treat cancer. It has been reported in several pre-clinical studies that DCA treatment results in significant suppression of tumor growth. However, in clinical investigation, the safety profile of DCA was a concern. Even so, Garon et al. (2014) who conducted a clinical trial with DCA on lung cancer patients, concluded that: “in the absence of a larger controlled trial, firm conclusions regarding the association between the patient’s adverse events

and DCA are unclear". They recommended that DCA should be considered with platinum-based chemotherapy in hypoxic tumors rather than as a single agent in advanced non-small cell lung cancer. DCA is believed to be a powerful molecule that warrants further investigation of its anti-cancer potential.

In this research project, the aim was to investigate the impact of DCA alone and in combination with the cytotoxic chemotherapeutic agents "Cisplatin, Gemcitabine and Camptothecin", the natural compound Frondoside A, the EGFR targeted therapies "Gefitinib or Erlotinib" on lung tumor growth and metastasis.

This research was addressed using two NSCLC cells namely A549 and LNM35 through the following objectives:

- To investigate the impact of DCA on
  - Cancer cell viability and colony growth *in-vitro*.
  - Cancer cell migration and invasion *in-vitro*.
  - Angiogenesis *in-vitro*.
  - Tumor growth and metastasis using the chick embryo CAM and the nude mice models *in-vivo*.
- To determine the safety profile of DCA by investigating the *in-vivo* toxicity on blood, kidney, and liver in the nude mice model.
- To investigate the impact of DCA in combination therapies

This pre-clinical study will pave the way for future pre-clinical and clinical studies combining DCA with clinically available drugs for better treatment of lung cancer. The outcomes of this study will be of great value to the UAE and to worldwide lung cancer patients.

## Chapter 2: Materials and Methods

### 2.1 Cell Culture and Reagents

NSCLC cells, A549 and LNM35, were maintained in RPMI-1640 medium (Hyclone, Cramlington, UK) in humidified incubator at 37°C and 5% CO<sub>2</sub>. The medium was supplemented with 1% of Penicillin-Streptomycin solution (Hyclone, Cramlington, UK) and 10% of Fetal bovine serum (Hyclone, Cramlington, UK). EndoGRO<sup>TM</sup> Human umbilical endothelial cells (HUVECs) (Millipore, Temecula, CA) were maintained in EndoGRO<sup>TM</sup>-VEGF complete media kit (Millipore, Temecula, CA) in humidified incubator at 37°C and 5% CO<sub>2</sub> in flasks coated with 0.2% Gelatin. The culture medium of all cells was changed every 3 days and cells were passed once a week when the culture reached 95% confluency.

DCA, Frondoside A Hydrate, Cisplatin, Camptothecin, Gemcitabine HCl, Erlotinib HCl and Gefitinib were purchased from Sigma-Aldrich (Saint Louis, MO). DCA was freshly dissolved before the start of any experiment in HyPure water (Hyclone, Cramlington, UK) to have a stock solution of 1M which was then diluted to the required concentrations for treatment. Generally, it was reported that DCA dissolved in water remains stable up to 60 days when stored in a refrigerator at +4°C (Cascone et al., 2013).

### 2.2 Cellular Viability

A549 and LNM35 cells were seeded at a density of 5000 cells/well into 96-well plate. After 24 hrs, cells were treated with increasing concentration of DCA (3.125-100 mM) in duplicate for 24, 48 and 72 hrs, whereas control cells were treated with drug vehicle (Hypure water) mixed with medium. At the indicated time points,

CellTiter-Glo® Luminescent Cell Viability assay (Promega Corporation, Madison, USA) was used to determine the effect of DCA on the cellular viability by quantifying the ATP that will be proportional to the number of the metabolically active cells. Upon the addition of this reagent, ATP will be released from the viable cells to the medium and used by the luciferase to convert the luciferin into oxyluciferin that is responsible for the luminescence (Figure 4). The luminescent signal was measured by the GloMax® Luminometer. Cellular viability was presented as a percentage (%) by comparing the viability of DCA-treated cells to the control cells, the viability of which is assumed to be 100%.

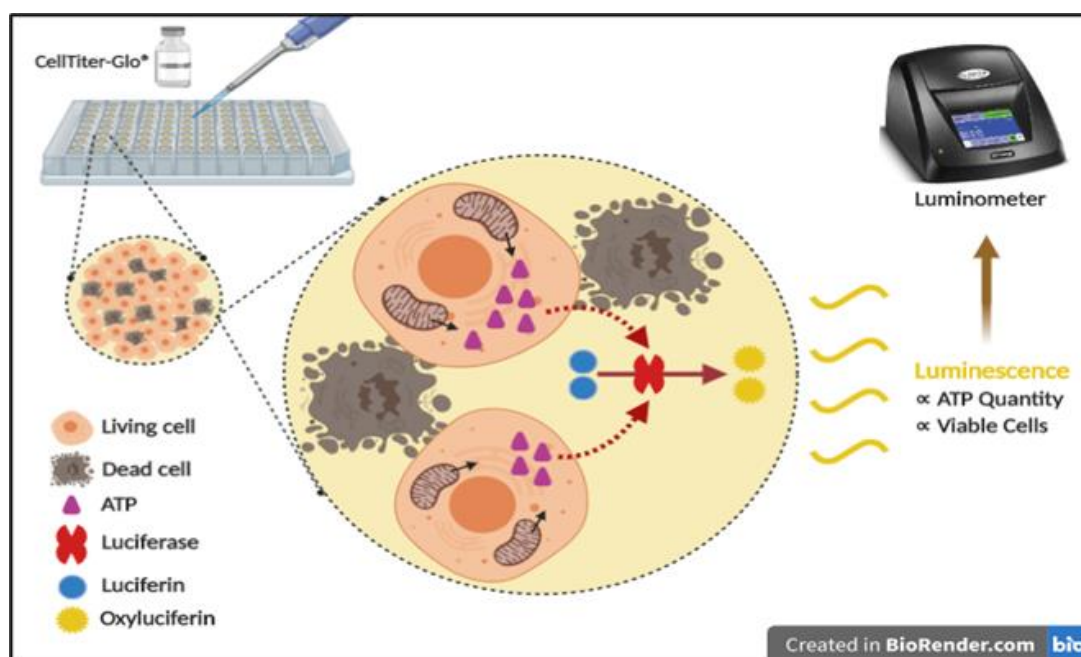


Figure 4: Schematic Representation for the Detection of Viable Cells using CellTiter-Glo® Luminescent Cell Viability Assay.

In the second set of experiments, cells were treated for 48 hrs with increasing concentration of Gefitinib and Erlotinib HCl (5 - 80  $\mu$ M). Additionally, cells were treated for 48 hrs with a combination of DCA and other anticancer agents, namely, Cisplatin, Camptothecin, Gemcitabine HCl, Frondoside A Hydrate, Gefitinib and

Erlotinib HCl. Cellular viability was determined using CellTiter-Glo<sup>®</sup> Luminescent Cell Viability assay and the GloMax<sup>®</sup> Luminometer. The viability was presented as a percentage (%) by comparing the viability of drug-treated cells with the control cells.

### **2.3 Clonogenic Assay**

Into a 6-well plate, A549 and LNM35 cells were seeded respectively at 50 and 100 cells/well. Cells were kept to grow into colonies for 7-14 days in humidified atmosphere at 37°C and 5% CO<sub>2</sub> with medium change every three days. Formed colonies were treated for 7 days with increasing concentrations of DCA (6.25-50 mM). Afterward, colonies were washed three times with 1X PBS, fixed and stained for 2 hrs with 0.5% crystal violet dissolved in 50% methanol (v/v). Finally, colonies were washed with 1X PBS, photographed and colonies with more than 50 cells were counted. Data were presented as colonies percentage (%) by comparing the DCA-treated colonies with the control colonies. Colony cell density was assessed by photographing the colonies in each group using an inverted phase contrast microscope (4x).

In the second set of experiments, formed colonies were treated for 7 days with a combination of DCA and Frondoside A Hydrate, DCA and Gefitinib or DCA and Erlotinib HCl. Data were presented as colonies percentage (%) by comparing the drug-treated colonies with the control colonies.

### **2.4 *In Ovo* Tumor Growth Assay**

Fertilized Leghorn eggs were incubated in the egg incubator set at temperature of 37.5°C and humidity of 50% for the first 3 days after fertilization. At the embryonic day 3 (E3), the chorioallantoic membrane (CAM) was dropped by drilling a small hole

in the eggshell opposite to the round, wide end followed by aspirating ~1.5 - 2 ml of albumin using 5 ml syringe with 18G needle. Then, a small window was cut in the eggshell above the CAM using delicate scissor and sealed with a semipermeable adhesive film (Suprasorb<sup>®</sup> F). The eggs were kept again in the egg incubator till the embryonic day 9 (E9) in which cancer cells were trypsinized, centrifuged and suspended in 80% Matrigel<sup>®</sup> Matrix (Corning, Bedford, UK) to have  $1 \times 10^6$  cells/100 $\mu$ L for A549 and  $0.3 \times 10^6$  cells/100 $\mu$ L for LNM35. A 100  $\mu$ L inoculum was added onto the CAM of each egg, for a total of 10-13 eggs per condition. At the embryonic day 11 (E11), formed tumors were treated topically by dropping 100  $\mu$ L of the DCA prepared in 0.9% NaCl for the first group or the drug vehicle for the control group. Treatment was repeated at E13 and E15. All the described steps were performed under aseptic conditions. Finally, at the embryonic day 17 (E17), embryos were humanely euthanized by topical addition of 10-30  $\mu$ L Pentobarbitone Sodium (300 mg/ml, Jurox, Auckland, New Zealand). Tumors were carefully extracted from the normal upper CAM tissues, washed with 1x PBS and weighted to determine the effect of DCA on tumor growth. Data were presented by comparing the average weight of tumors in the control group and DCA-treated group. Drug toxicity was assessed by comparing the percentage of alive embryos in the control and DCA-treated groups at the end of the experiment. Alive embryos were determined by checking the voluntary movements of the embryos in addition to the integrity and pulsation of the blood vessels.

This assay is a randomly assigned unblinded assay that was done according to the protocol approved by the animal ethics committee at the United Arab Emirates University. According to the European Directive 2010/63/EU on protection of animals

used for scientific purposes, experiments involved using chicken embryos on and before E18, don't require approvals from the institutional Animal Care and Use Committee (IACUC).

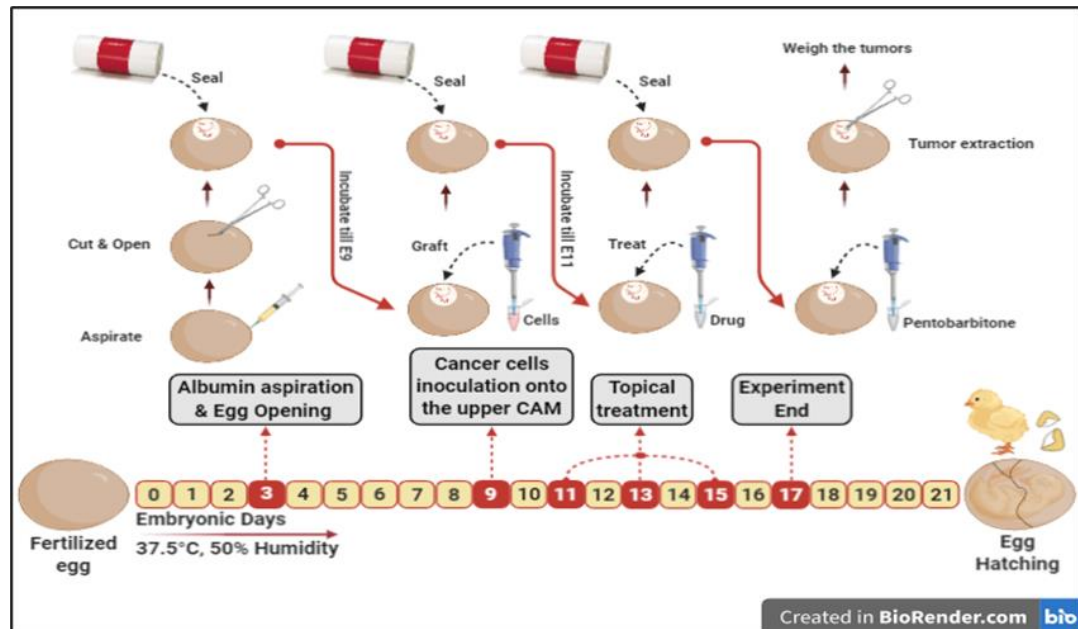


Figure 5: Schematic Representation of the *In-Ovo* Tumor Growth Assay.

## 2.5 Tumor Growth and Metastasis Assay

The animal experiments were performed according to the protocol approved by the animal ethics committee and the Institutional Animal Care at the College of Medicine and Health Sciences, UAE university. Six to eight weeks old athymic NMRI male nude mice (nu/nu, Charles River, Germany) were housed in filtered-air laminar flow cabinets and handled under aseptic conditions. A549 cells ( $5 \times 10^6$  cells / 200  $\mu$ L PBS) and LNM35 cells ( $0.4 \times 10^6$  cells / 200  $\mu$ L PBS) were injected subcutaneously into the lateral flank of the nude mice. Ten days later, when tumors had reached the volume of approximately 50 mm<sup>3</sup>, animals with A549 xenografts were divided randomly into three groups of 9-10 mice each. These groups were treated orally every day (5 days/week) with DCA 50 mg/kg or 200 mg/kg or drug vehicle for 38 days. On

the other hand, animals with LNM35 xenografts were treated orally every day (5 day/week) with DCA 200 mg/kg or drug vehicle for 14 days and DCA 500 mg/kg or drug vehicle for 24 days. Tumor dimensions and animal weights were checked every three or four days. In addition, the physical signs and behavior were checked every day. Tumor volume was calculated using the formula  $V=L \times W^2 \times 0.5$  knowing that L stands for the length and W stands for the width of the tumor. At the end of the experiments, animals were anaesthetized, sacrificed by cervical dislocation and tumors were removed and weighted. Effect of DCA on tumor growth was presented by comparing the average tumor weight at the end of the experiment between the control group and DCA-treated group. It was also assessed by comparing the tumor volume between the control and DCA-treated groups throughout the experiment. Blood samples were collected from each mouse and analyzed using SCIL VET ABC™ Animal Blood Counter for complete blood count. In addition, blood plasma were separated by centrifugation for biochemical analysis. To study the impact of DCA on metastasis, axillary lymph nodes were excised and weighted from the animals with LNM35 xenografts at the end of the experiment.

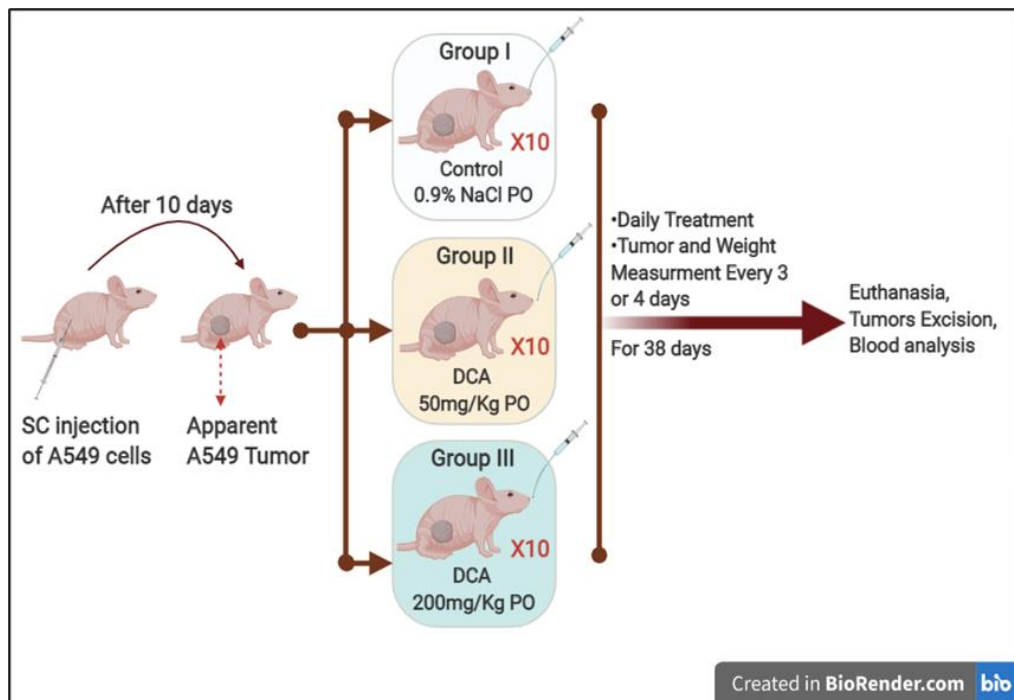


Figure 6: Schematic Representation of Xenografting A549 Cells into the Nude Mice and the Oral treatment with DCA 50 mg/Kg and 200 mg/Kg.

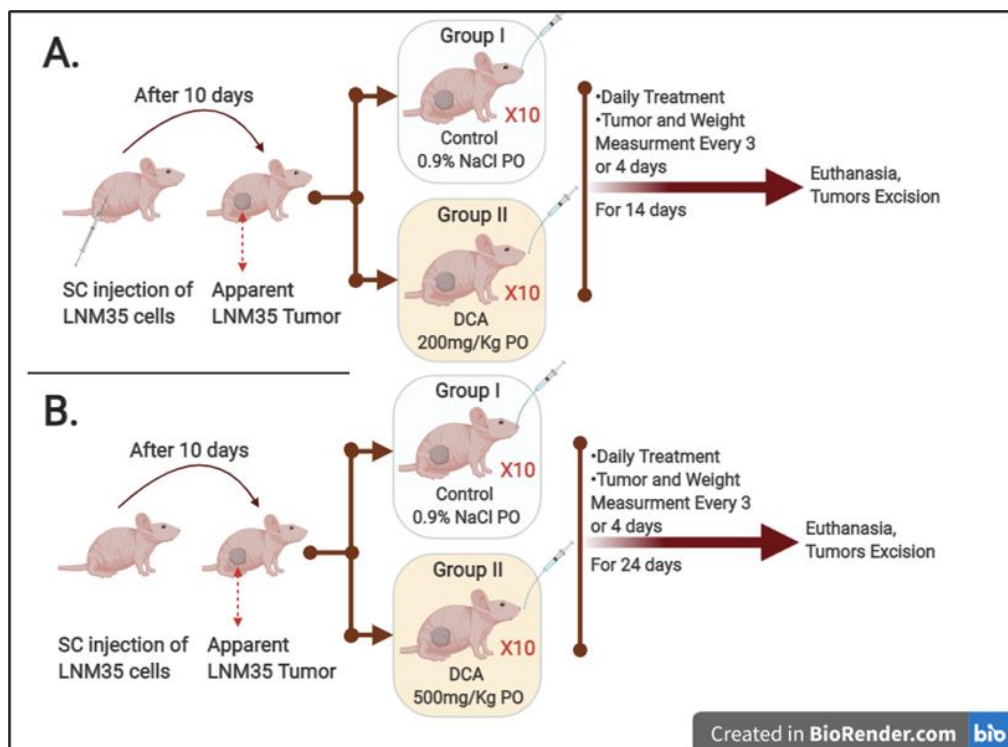


Figure 7: Schematic Representation of Xenografting LNM35 Cells into the Nude Mice and the Oral Treatment with DCA 200 mg/Kg (A) and DCA 500 mg/Kg (B).

## 2.6 Vascular Tube Formation Assay

Matrigel<sup>®</sup> Matrix (Corning, Bedford, UK) was thawed and 40-50  $\mu$ L was added to the wells of 96-well plate for coating. In order for the Matrigel to solidify, the plate was kept in a humidified incubator at 37°C and 5% CO<sub>2</sub> for 1 hour. HUVECs were trypsinized and seeded on the coated plate at a density of  $2.5 \times 10^4$  cells / 100  $\mu$ L / well in the presence and absence of different concentrations of DCA. After 8 hrs of incubation, the tube networks at the different wells were photographed using an inverted phase contrast microscope. Impact of DCA on the ability of HUVECs to form capillary-like structures was assessed by measuring the total lengths of the formed tubes in the control and DCA-treated wells. Measurement of total tube lengths was done manually and through an online image analysis software developed by Wimasis. The effect of the different concentrations of DCA on the viability of HUVECs was determined using CellTiter-Glo<sup>®</sup> Luminescent Cell Viability assay (Promega Corporation, Madison, USA) as previously described in the cellular viability section.

## 2.7 HUVEC Spheroids Sprouting Assay

HUVEC spheroids were prepared by firstly staining the cells by incubating 190,000 cells with 2  $\mu$ M solution of CellTracker<sup>™</sup> Green CMFDA Dye (Molecular probes, Invitrogen, UK) for 30 minutes in humidified incubator set at 37°C and 5% CO<sub>2</sub> followed by centrifugation for 5 minutes and removal of supernatant. HUVECs pellet was suspended with supplemented HUVEC medium (5 ml) mixed with methocel solution (1.25 ml), that should be prepared earlier (Tetzlaff & Fischer, 2018). Then, 25  $\mu$ l of the cell suspension were pipetted onto the cover of petri dish. Approximately,

50 drops were pipetted in each petri dish, as shown in Figure 8A. Finally, Drops were kept upside down for 24 hrs in humidified incubator set at 37°C and 5% CO<sub>2</sub>.

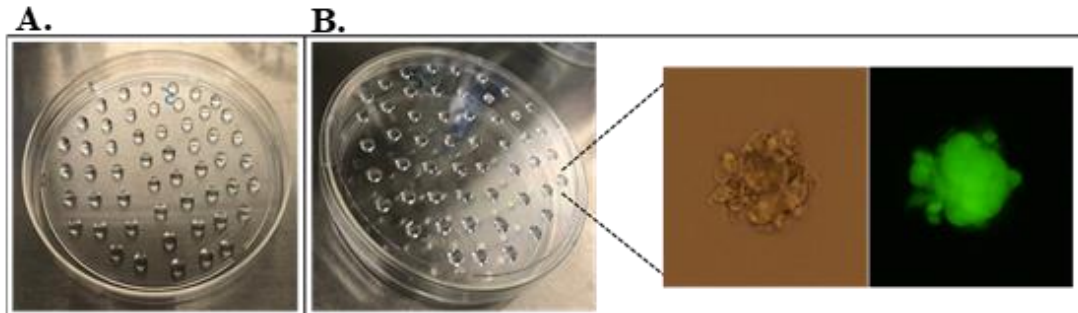


Figure 8: Preparation of Hanging Drops for Spheroid Preparation. (A) Petri dish with drops before kept them upside down. (B) Representative image of HUVEC spheroid in a hanging drop after 24 hrs of upside-down incubation.

Formed spheroids in each dish (~50 spheroids) (Figure 8B) were collected separately with 1x PBS and centrifuged at 150xg for 5 minutes, no brake. In the meantime, collagen I working solution was prepared on ice by gentle mixing of rat tail collagen I stock (1500  $\mu$ L) with 10X medium 199 (150  $\mu$ L) (Sigma-Aldrich, saint Louis, MO) and ice-cold sterile 1N NaOH (34  $\mu$ L) ending with red color. Each spheroids pellet was layered with methocel solution having 4% FBS (0.25 ml), collagen I working solution (0.25 ml) and 60  $\mu$ l of basal medium or VEGF 30ng/ml or DCA 25 mM or combination of both. Immediately after gentle mixing, the mixture was added to a pre-warmed 24-well plate and incubated in humidified incubator set at 37°C and 5% CO<sub>2</sub> for 24 hrs allowing for collagen polymerization and spheroids sprouting. After 24 hrs, spheroids were captured using inverted microscope with 20x magnification. Sprouts length in 12 spheroids in each condition was measured using ImageJ.

## 2.8 Wound Healing Motility Assay

A549 and LNM35 cells were seeded at a density of  $1 \times 10^6$  cells/well into a 6-well plate. After 24 hrs, a scratch was made through the confluent monolayer by using a 200  $\mu$ L tip. After that, the cells were washed twice with 1x PBS followed by the addition of supplemented fresh medium having drug vehicle or DCA. At the top of the plate, two places were marked to monitor the decrease in the wound size over time, using an inverted microscope at objective 4x (Olympus 1X71, Japan). The plates were incubated in humidified atmosphere at 37°C and 5% CO<sub>2</sub> and the wound width was measured at 0, 2, 6 and 24 hrs after incubation. Migration distance was expressed as the average of the difference between the measurements at time zero and the 2, 6 and 24 hrs time periods.

## 2.9 Matrigel Invasion Assay

The effect of DCA on the invasiveness of A549 and LNM35 cancer cells was investigated using the Matrigel<sup>®</sup> Invasion Chamber assay (Corning, Bedford, USA). This assay utilizes a 24-well plate with inserts composed of semipermeable membranes with 8  $\mu$ m pores coated with Matrigel. The invasive cells can degrade the matrix and penetrate through the insert pores to the other side. Following the manufacture's protocol, 0.5 mL RPMI-1640 medium, supplemented with 10% FBS, was added to the bottom chambers. After that, cancer cells were seeded at a density of  $1 \times 10^5$  cells / 0.5 mL into the upper chambers in medium lacking Fetal Bovine Serum in the presence and absence of DCA. The plate was kept in humidified incubator at 37°C and 5% CO<sub>2</sub> for 24 hrs after which the non-penetrating cells in the upper chambers were removed by rubbing the area gently with a cotton swab. Then, the

semipermeable membrane was removed using a very fine scissor and the invading cells were detected using CellTiter-Glo® Luminescent Cell Viability assay (Promega Corporation, Madison, USA) as previously described in the cellular viability section. The effect of DCA on cellular invasion was presented as a percentage (%) by comparing the invading cells in the presence of DCA with the control.

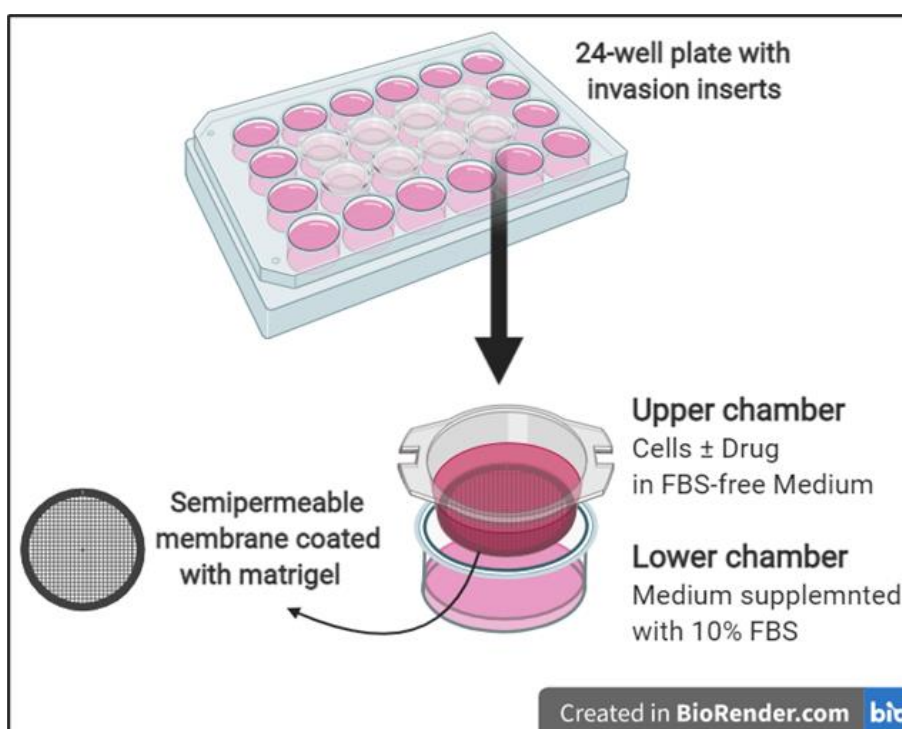


Figure 9: Schematic Representation of the Invasion Chamber Assay.

## 2.10 Statistical Analysis

Apart from the *in ovo* assay and experiments on nude mice, each experiment was carried out for at least three independent times. Data were expressed as mean ± S.E.M. Statistical analysis was performed using GraphPad Prism version 8.3.1 for Windows (GraphPad Software, San Diego, California USA). Unpaired t-test was used to assess the difference between two groups. One-way ANOVA followed by Dunnett's multiple comparison test were used to compare 3 or more groups to control group.

Additionally, One-way ANOVA followed by Tukey's multiple comparison test were used for the combination experiments. \*P <0.05, \*\*P <0.01. \*\*\*P <0.001. \*\*\*\*P <0.0001 indicate significant differences.

## Chapter 3: Results

### 3.1 Effect of DCA on Cellular Viability and Colony Growth of NSCLC Cell Lines

The effect of increasing concentration of DCA (6.25-100 mM) was investigated on two NSCLC cell lines, namely, A549 and LNM35. As shown in Figure 10, DCA reduced the viability of A549 (Figure 10A) and LNM35 (Figure 10B) in a concentration and time-dependent manner. The half maximal inhibitory concentration (IC<sub>50</sub>) of DCA at 48 hours is approximately 25 mM for both cell lines.

For further assessment of the anticancer effect of DCA, its impact was investigated on the growth of pre-formed colonies of A549 and LNM35 cell lines. Toward this, both cell lines were grown at specific density for 1 week to form colonies and then treated with increasing concentration of DCA for another 1 week. As shown in Figure 10, DCA caused a concentration-dependent reduction in the percentage of colonies for both cell lines with higher sensitivity shown in LNM35 colonies (Figure 10D) compared to A549 colonies (Figure 10C). These results confirm the anticancer effect of DCA *in-vitro*.

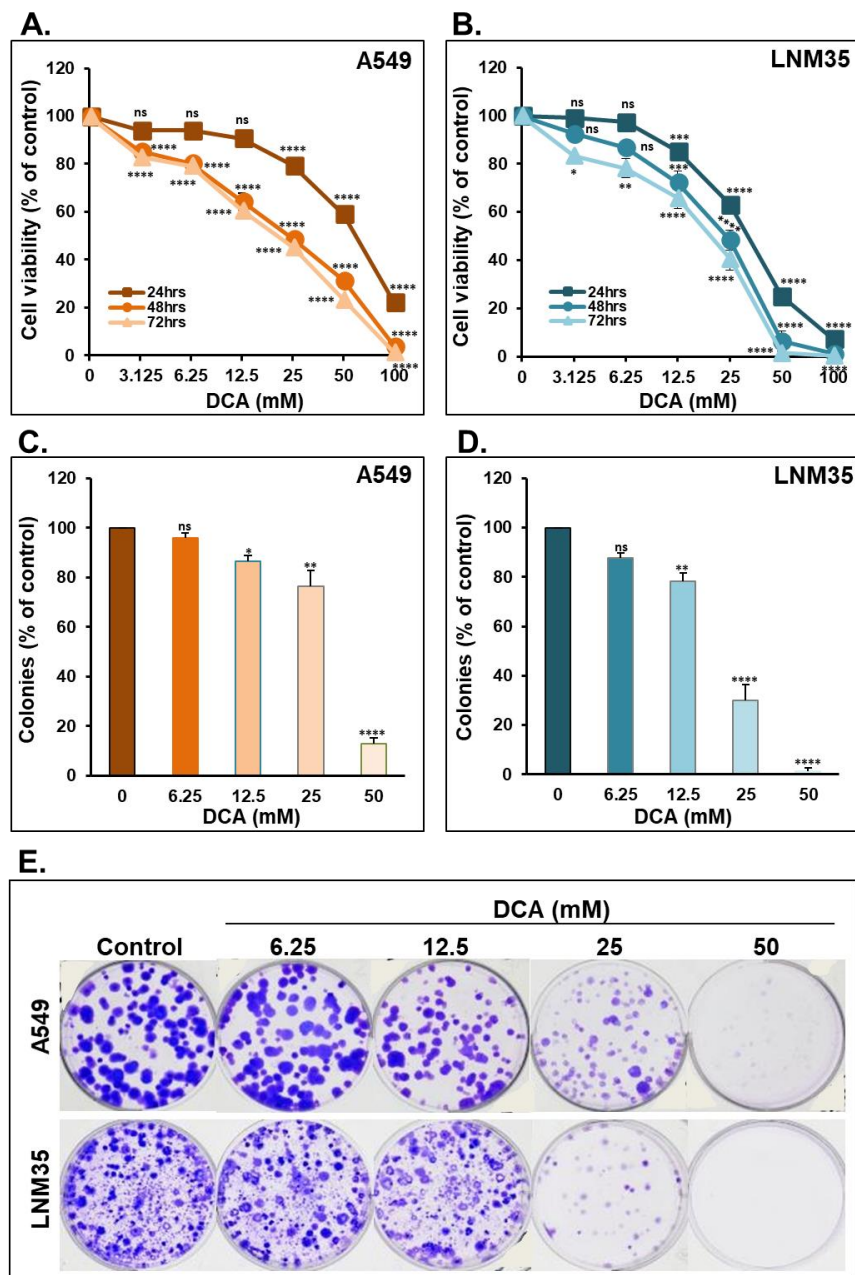


Figure 10: Effect of DCA on NSCLC Cells Viability and Colony Growth. Exponentially growing A549 (A) and LNM35 (B) cancer cells were incubated in the absence or presence of increasing concentrations of DCA (3.125-100 mM) for 24, 48 and 72 hrs. Cellular viability was assessed as described in the Materials and Methods. Shapes represent means; bars represent S.E.M. A549 (C) and LNM35 (D) cancer cells were grown for 7 days to form colonies that were treated with different concentrations of DCA (6.25-50 mM) for 7 days after which colonies were fixed, stained and counted as described in the Materials and Methods. (E) Representative pictures of the control and DCA-treated colonies are shown for A549 and LNM35 cancer cells. Experiments were repeated at least three independent times. Results are presented as percent colonies (mean  $\pm$  S.E.M.) of treated cells compared to control. ns Not significant. \*Significantly different at  $<0.05$ . \*\*Significantly different at  $<0.01$ . \*\*\*Significantly different at  $<0.001$ . \*\*\*\*Significantly different at  $<0.0001$ .

### **3.2 Effect of DCA on the Growth of NSCLC Tumor Xenografts in the Chick Embryo CAM and Nude Mice *In-Vivo***

To confirm the pharmacological relevance of the *in-vitro* results, the anticancer effect of DCA was evaluated *in-vivo* using chick embryo CAM assay. A549 and LNM35 xenografted tumors on the CAM were treated with 50 mM of DCA every 48 hrs for 1 week. At E17, tumors were recalled from the upper CAM and weighed. As observed in Figure 11, 50 mM of DCA significantly reduced the growth of A549 tumor xenografts (Figure 11A) by approximately 40% while it didn't show a significant reduction in the growth of LNM35 tumor xenografts (Figure 11B). Therefore, 100 mM of DCA was investigated on LNM35 tumor xenografts and it significantly reduced the growth by approximately 40% (Figure 11C). Toxicity was also assessed by comparing the percentage of alive embryos in the control and DCA-treated groups. At E17, DCA showed no cytotoxicity as the percentage of alive embryo was similar with control and DCA treatment (Figures 11D, E, F).

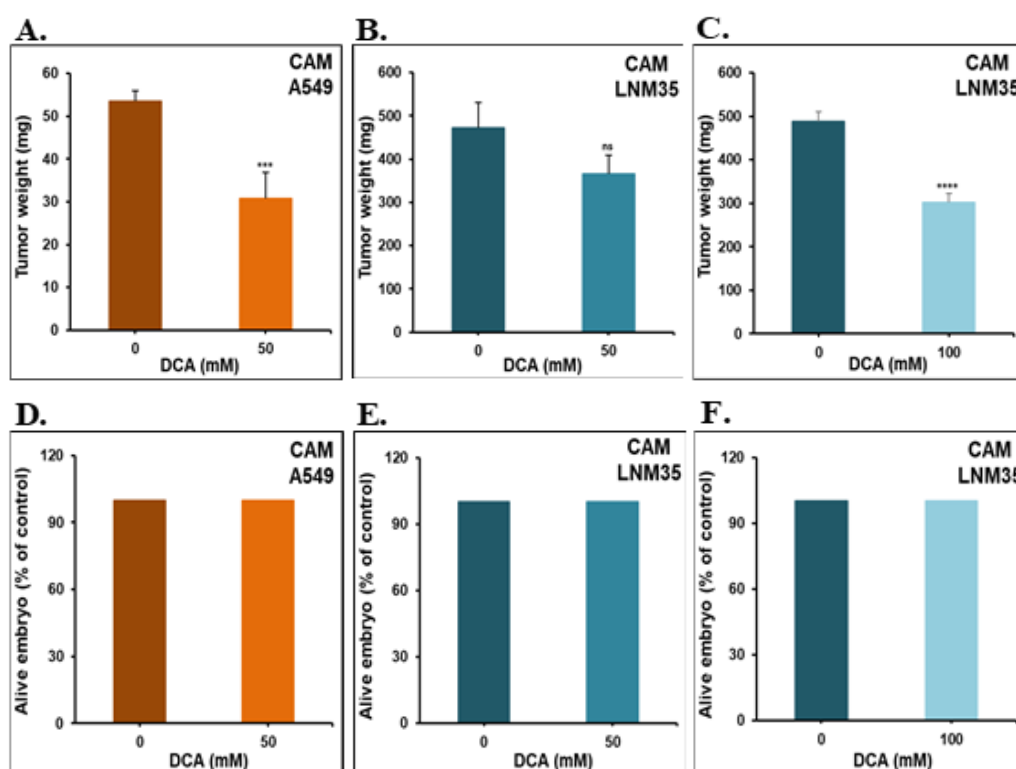


Figure 11: Effect of DCA on the growth of A549 and LNM35 tumor xenografts in the chick embryo CAM *in-vivo*. (A) Tumor weight of A549 cancer cells xenografted on the CAM at a density of 1 million cells after treatment with drug vehicle (0.9% NaCl) or DCA (50 mM) for 1 week. (B, C) Tumor weight of LNM35 cancer cells xenografted on the CAM at a density of 0.3 million cells after treatment with drug vehicle (0.9% NaCl) or DCA (50 mM & 100 mM). (D) Percentage of alive embryo in the control and DCA-treated A549 xenograft. (E, F) Percentage of alive embryo in the control and DCA-treated LNM35 xenograft. Columns are means; bars are S.E.M. \*\*\*Significantly different at <0.001. \*\*\*\*Significantly different at <0.0001.

The impact of DCA on tumor xenografts was also evaluated *in-vivo* using athymic mice inoculated with A549 and LNM35 cells. The median lethal dose (LD50) of DCA was reported to be 4.5 g/kg and 5.5 g/kg in rats and mice, respectively (Anand et al., 2014; Laug, 2016). Therefore, the mice with A549 tumor xenografts were treated orally everyday (5 days/week) with 50 mg/kg and 200 mg/kg of DCA for 38 consecutive days. Treatment with DCA (50 mg/kg) didn't cause a significant reduction in the volume of A549 tumor xenografts while DCA (200 mg/kg) significantly reduced the volume by approximately 45% (Figure 12A). A similar difference was also observed in tumor weight at the end of the experiment (Figure 12B). There were no

obvious signs of toxicity or any manifestation of undesirable effects of DCA on animal behavior, body weight (Figure 12C), blood components (Figure 12D), liver and kidney function parameters (Data not shown).

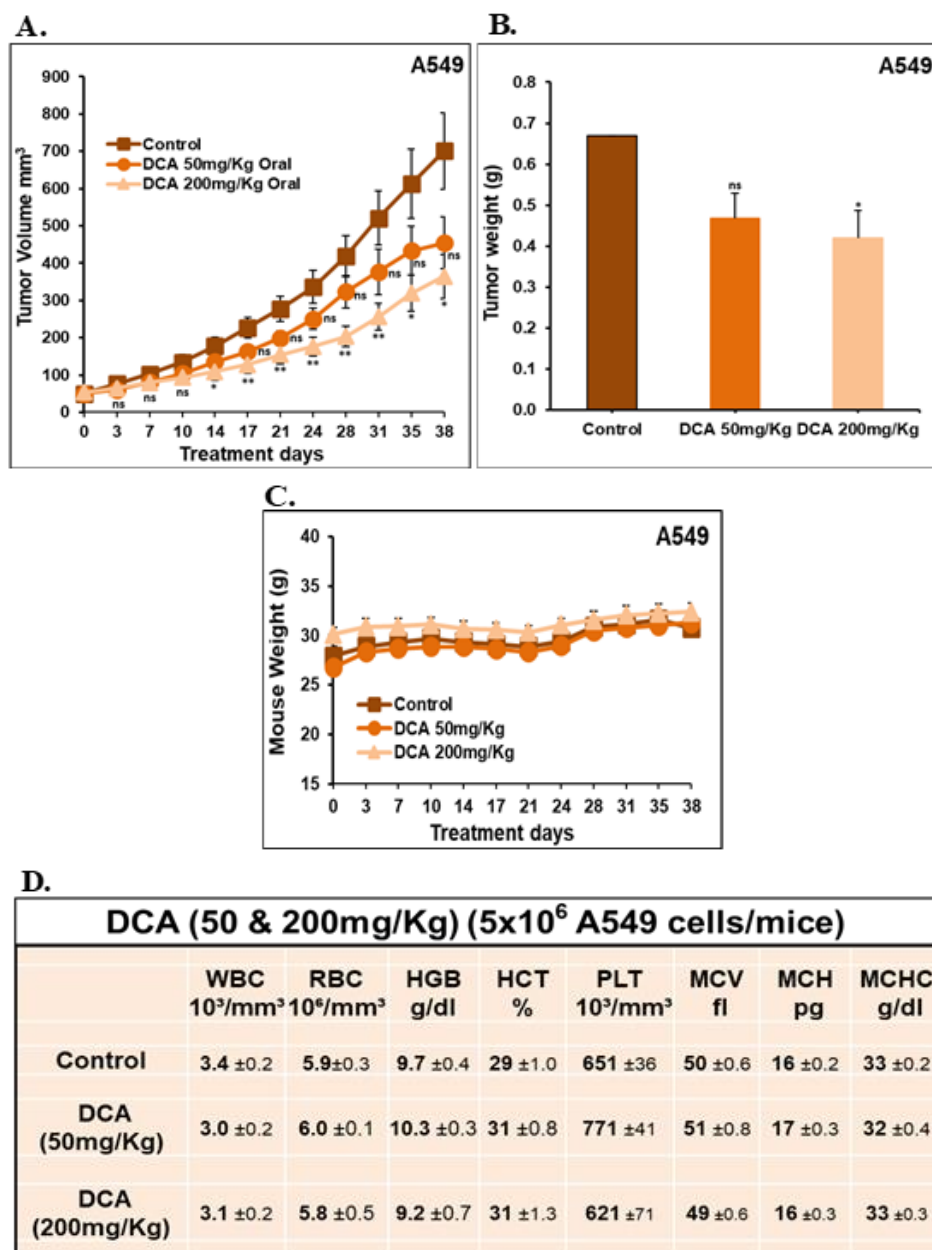


Figure 12: Effect of DCA on the Growth of A549 Xenografted in Nude Mice *In-Vivo*. (A) Tumor volume of A549 xenograft inoculated subcutaneously in nude mice and treated with DCA (50 & 200 mg/kg) orally or control carrier solution alone for a total of 38 days. (B) Tumor weight obtained from the same control and DCA-treated nude mice. (C) Average of the mice body weight through the treatment days. (D) Mice blood samples were analyzed for complete blood count parameters. Results represent mean  $\pm$  S.E.M. of 9-10 mice/group. \*Significantly different at  $<0.05$ . \*\*Significantly different at  $<0.01$ .

On the other hand, the growth of LNM35 tumor xenografts was monitored and the mice were treated orally with 200 mg/kg and 500 mg/kg of DCA every day (5 days/week) for 14 and 24 consecutive days, respectively. Treatment with DCA (200 mg/kg) didn't show any reduction in the volume of LNM35 tumor xenografts (Figure 13A) while DCA (500 mg/kg) significantly decreased the tumor volume by nearly 75% (Figure 13B). Almost similar differences were seen in tumors weight at the end of the experiments (Figure 13C, D). No signs of toxicity were observed on animal behavior and detected on mice weight (Figure 13E, F), blood components (Figure 13G), liver and kidney function (Data not shown). Taken together, these results suggest the higher sensitivity of A549 cancer cells to DCA compared to LNM35 cancer cells *in-vivo*.

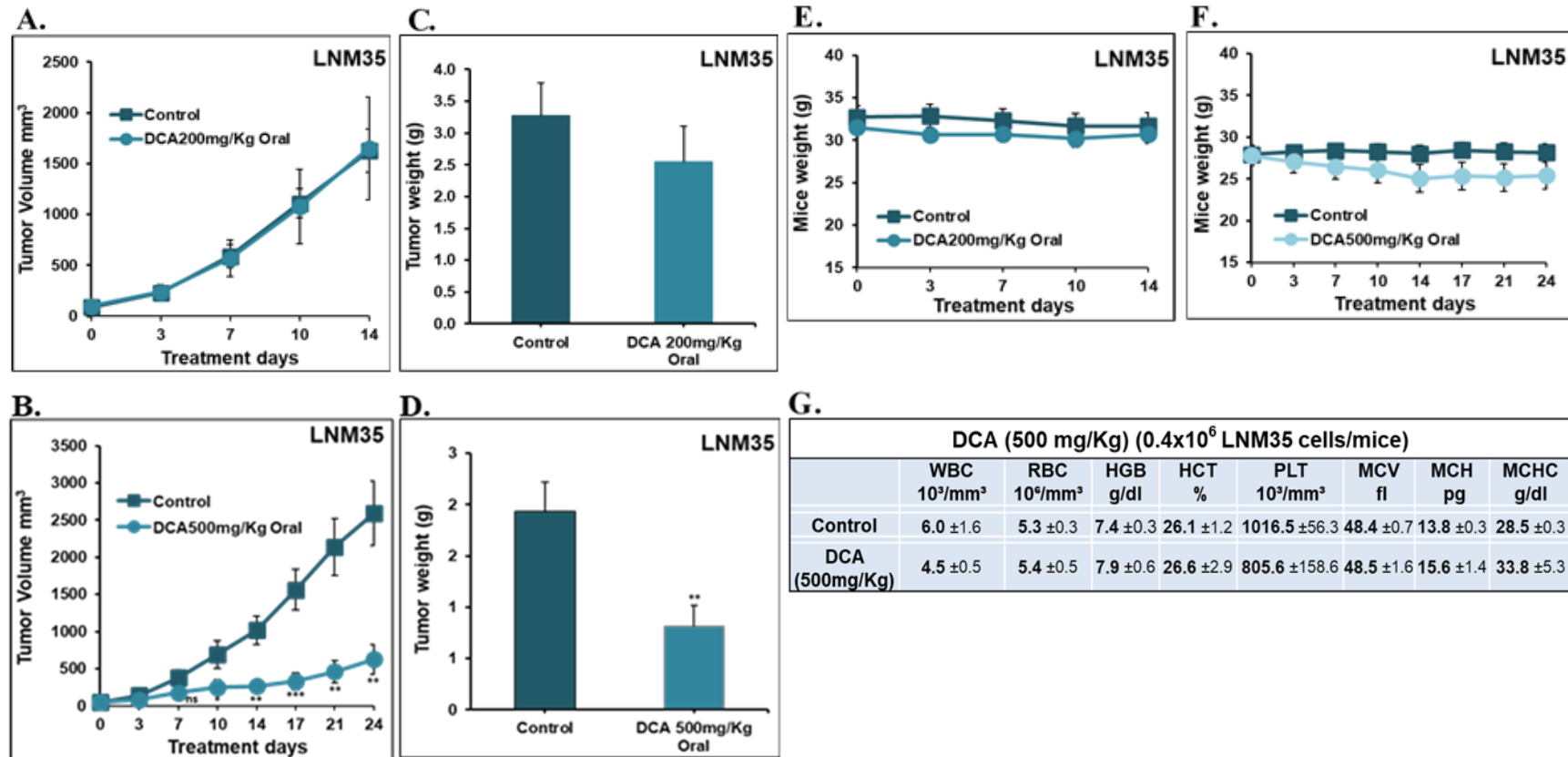


Figure 13: Effect of DCA on the Growth of LNM35 Xenografted in Nude Mice *In-Vivo*. (A, B) Tumor volume of LNM35 xenograft inoculated subcutaneously in nude mice and treated respectively with DCA (200 & 500 mg/kg) orally or control carrier solution alone daily for a total of 14 and 24 days. (C, D) Tumor weight obtained from the same control and DCA-treated nude mice. (E, F) Average of the mice body weight of throughout the treatment days. (G) Mice blood samples were analyzed for complete blood count parameters. Results represent mean ± S.E.M. of 9-10 mice/group. \*\*Significantly different at <0.01. \*\*\*Significantly different at <0.001.

### **3.3 Effect of DCA on the Formation of Capillary-Like Structures and Sprouting by HUVECs *In-Vitro***

Angiogenesis is one of the cancer hallmarks that ensures the supply of nutrients and oxygen in order for the cancer cells to grow and spread. Impact of DCA on angiogenesis was investigated *in-vitro* by using HUVECs that have the ability to form capillary-like structures when seeded on Matrigel. As shown in Figure 14A, HUVECs formed an organized capillary-like structures in the absence of DCA and this organization was disturbed after DCA addition. Tubes length were measured manually (Figure 14B) and by using Wimasis Image Analysis (Figure 14C) and it was found that 25 mM of DCA was able to significantly inhibit the HUVECs capacity to form the threaded structures by almost 40%. This inhibition was observed with concentration that didn't show any reduction in HUVECs viability (Figure 14D).

In the sprouting assay, spheroids of HUVECs were embedded in a 3D collagen matrix in the presence and absence of VEGF 30 ng/ml, DCA 25 mM or Combination of VEGF and DCA. As shown in Figure 15A, B, sprouts formed in the presence of VEGF was inhibited by DCA 25 mM. Total sprouts length were measured and it was found that total length was significantly increased in the presence of VEGF and DCA significantly decreased the sprout length induced by VEGF. This inhibition was observed with a concentration that didn't show any reduction in HUVECs viability (Figure 15C).

These data suggest that inhibition of tumor angiogenesis could be a potential mechanism beyond the anticancer effects of DCA.

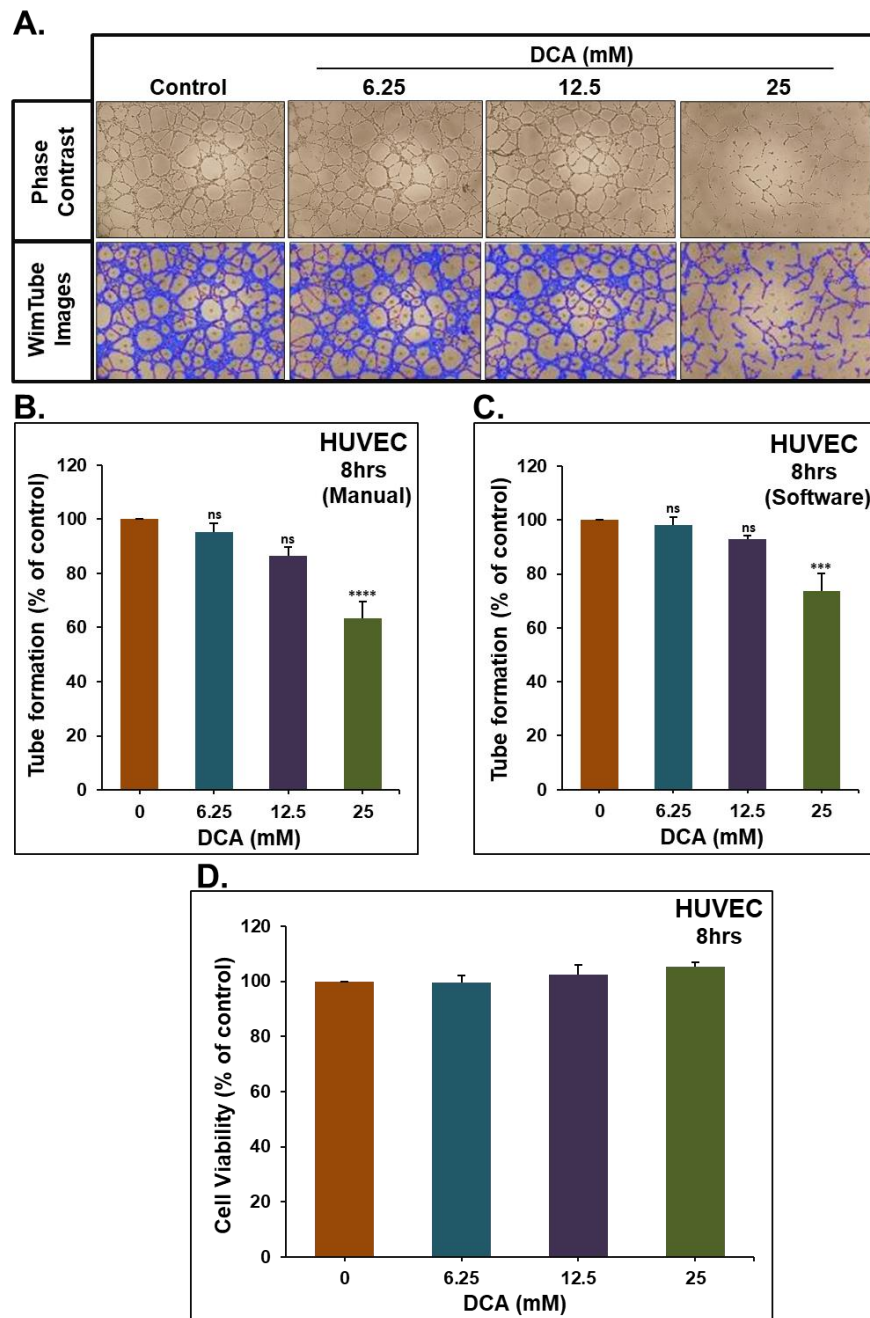


Figure 14: Effect of DCA on the Formation of Capillary-Like Structures by HUVECs *In Vitro*. (A) Forms of angiogenesis induced in HUVEC cultured on Matrigel matrix in 96-well plate in the absence and presence of different concentrations of DCA. An inverted microscope was used for contrast photo and Wimasis software was used to clarify the pictures. (B, C) Quantification of tubular angiogenesis induced in HUVEC cells cultured in the absence and presence of DCA (6.25 - 25 mM) manually and by using Wimasis software, respectively. (D) HUVEC cells viability was determined as described in the Material and Methods in the absence and presence of DCA (6.25 - 25 mM). Experiments were repeated for at least 3 independent times. Columns represent means; bars represent S.E.M. \*\*\*Significantly different at  $<0.001$ . \*\*\*\*Significantly different at  $<0.0001$ .

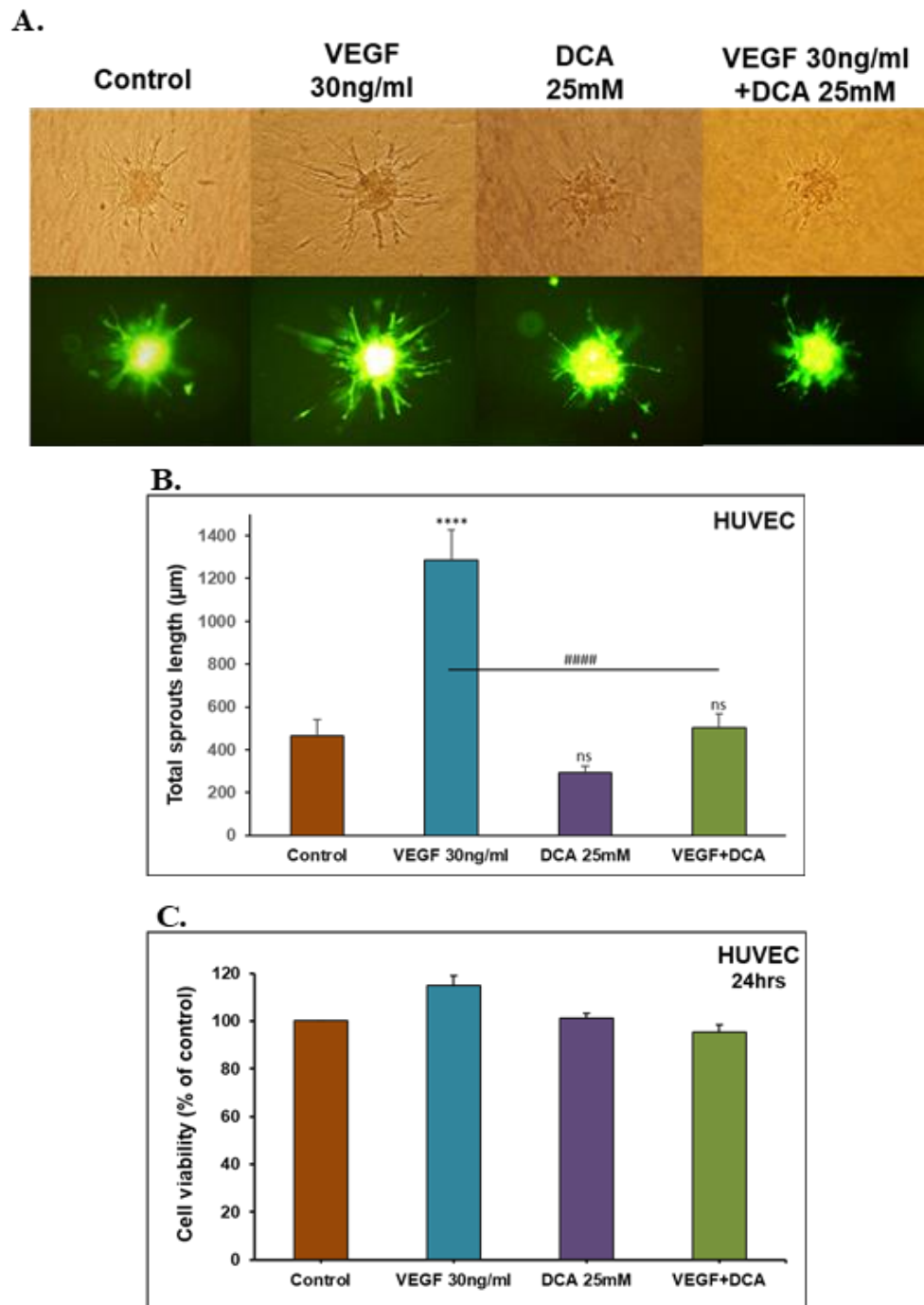


Figure 15: Effect of DCA on the Formation of Sprouts by the Embedded HUVECs Spheroids *In-Vitro*. (A) Representative images of pre-dyed HUVEC spheroids after 24 hrs of embedding in collagen matrix in the presence of VEGF 30 ng/ml, DCA 25 mM or VEGF+DCA. An inverted microscope at 20X magnification was used. (B) Average of total sprouts length from different spheroids per condition. (C) HUVEC cells viability was determined as described in the Material and Methods under similar conditions of embedded spheroids. Experiments were repeated 2 independent times. Columns represent means; bars represent S.E.M. \*\*\*\*Significantly different at <0.0001. ####Significantly different at <0.0001.

### 3.4 Effect of DCA on NSCLC Metastasis *In-Vivo* and Invasion and Migration *In-Vitro*

Metastasis is a multistep process that comprised of cells detachment from the primary tumor, cells migration to the adjacent tissues followed by cells invasion into blood or lymphatic system till the colonization of these cells in the distant organs. Effect of DCA on metastasis in mice xenografted with the highly metastatic lung cancer cells, namely, LNM35 was evaluated by checking the weight and incidence of axillary lymph nodes in the control and DCA-treated group. DCA decreases the growth of lymph node metastases without reaching a statistical significance (Figure 16A). In addition, it didn't affect on the incidence of lymph node metastases (Figure 16B).

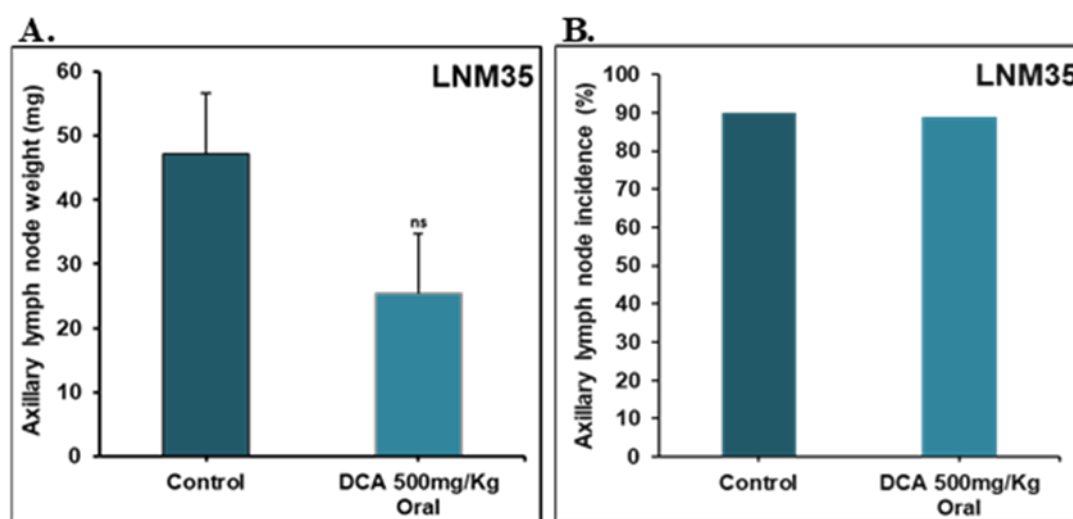


Figure 16: Effect of DCA on NSCLC Metastasis *In-Vivo*. (A) Weight of lymph node with LNM35 metastases in control and DCA-treated group (500 mg/kg PO). Results represent mean  $\pm$  S.E.M of 9-10 mice/group. (B) Percentage of mice with LNM35 lymph node metastases in control and DCA-treated group.

*In-vitro* Boyden chamber invasion assay and migration assay were used to evaluate the ability of DCA to inhibit A549 and LNM35 cells invasion and migration. 6.25 mM and 12.5 mM of DCA failed to inhibit cellular invasion of LNM35 (Figure

17A) and A549 (Figure 17B). Similarly, these concentrations failed to inhibit cellular migration of both cell lines (Figure 17C, D, E, F).

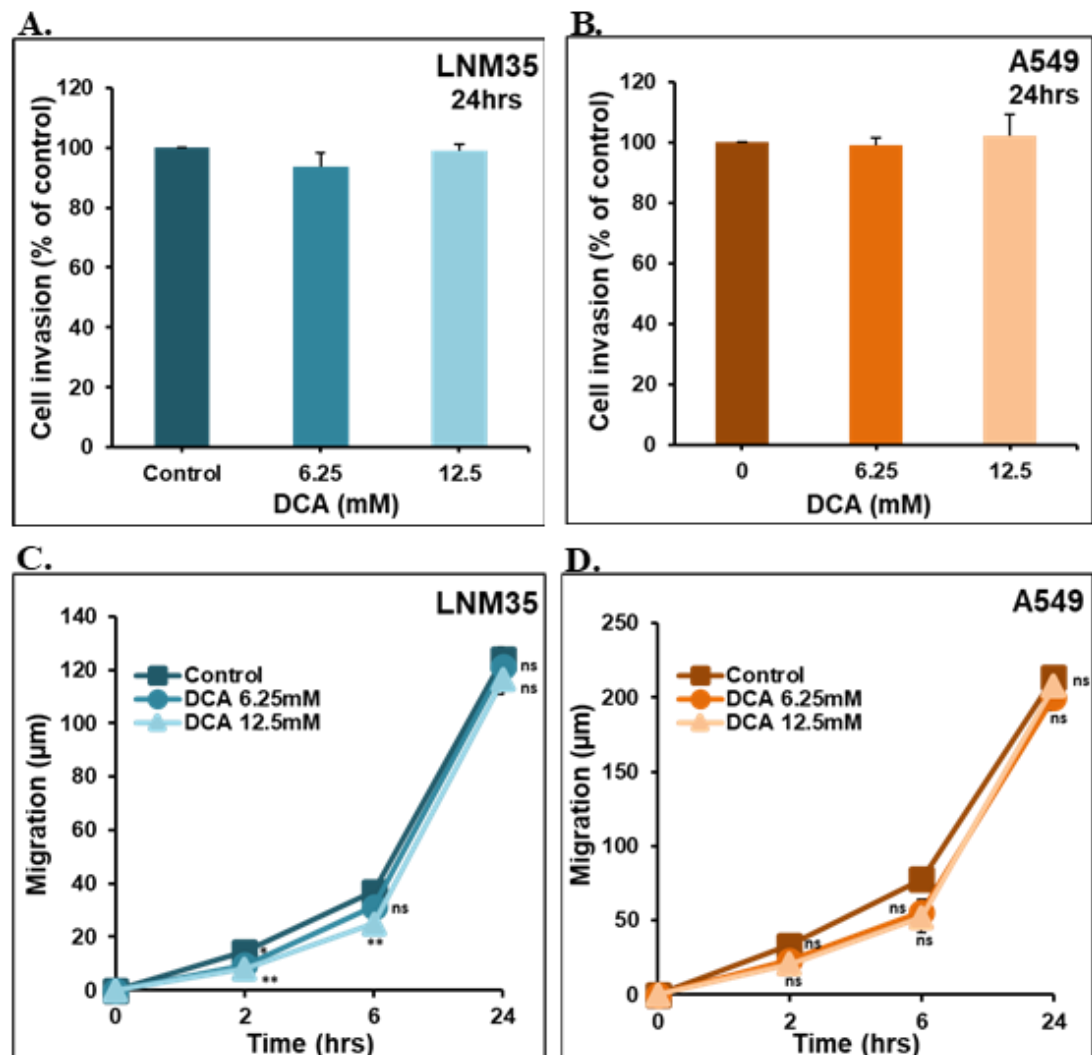
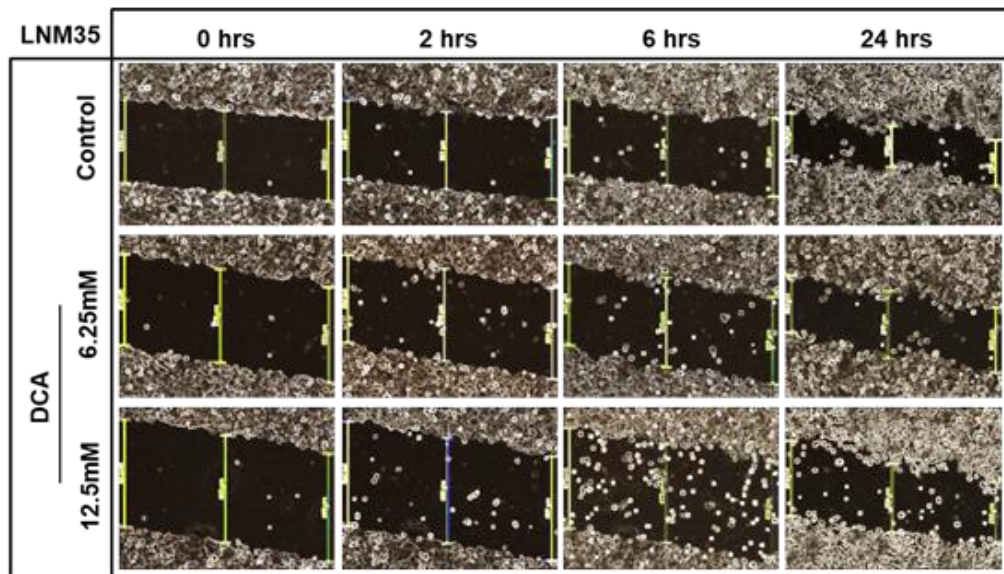


Figure 17: Effect of DCA on NSCLC Invasion and Migration *In-Vitro*. Using Boyden chamber assay, LNM35 (A) and A549 (B) cells were incubated for 24 hrs in the absence and presence of DCA (6.25, 12.5 mM). Cells that invaded into the Matrigel and cross the 8  $\mu\text{m}$  pores were determined as described in the Materials and Methods. Scratches were introduced in confluent monolayers of LNM35 cells (C) and A549 cells (D) cultured in 6-well plate in the absence and presence of DCA (6.25, 12.5 mM). Pictures of induced scratches in the confluent monolayers of LNM35 cells (E) and A549 cells (F) in the presence and absence of different concentrations of DCA at 0, 2, 6 and 24 hrs. An inverted microscope with 4X magnification was used to measure the average distance that cells migrated from the edge of the scrapped area for 2, 6, 24 hrs. All experiments were repeated for at least 3 independent times. Columns or Shapes are means; bars are S.E.M. ns Not significant. \*Significantly different at  $<0.05$ . \*\*Significantly different at  $<0.01$ .

E.



F.

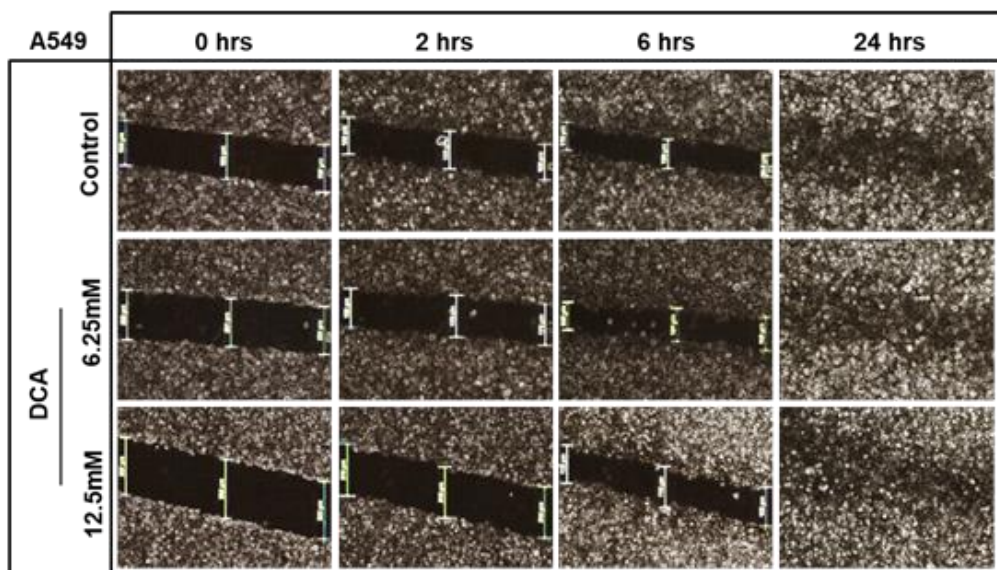


Figure 17: Effect of DCA on NSCLC Invasion and Migration *In-Vitro*. Using Boyden chamber assay, LNM35 (A) and A549 (B) cells were incubated for 24 hrs in the absence and presence of DCA (6.25, 12.5 mM). Cells that invaded into the Matrigel and cross the 8  $\mu$ m pores were determined as described in the Materials and Methods. Scratches were introduced in confluent monolayers of LNM35 cells (C) and A549 cells (D) cultured in 6-well plate in the absence and presence of DCA (6.25, 12.5 mM). Pictures of induced scratches in the confluent monolayers of LNM35 cells (E) and A549 cells (F) in the presence and absence of different concentrations of DCA at 0, 2, 6 and 24 hrs. An inverted microscope with 4X magnification was used to measure the average distance that cells migrated from the edge of the scrapped area for 2, 6, 24 hrs. All experiments were repeated for at least 3 independent times. Columns or Shapes are means; bars are S.E.M. ns Not significant. \*Significantly different at <0.05. \*\*Significantly different at <0.01 (Continued).

### **3.5 Effect of DCA in Combination with Chemotherapeutic Agents on the Viability of NSCLC Cells**

To further evaluate the therapeutic potential of DCA, impact of its anti-cancer effects was investigated on the activity of major chemotherapeutic drugs, namely, Cisplatin, Camptothecin and Gemcitabine. Treatment of the cells for 48 hrs with 25 mM of DCA failed to enhance the anti-cancer effects of Cisplatin (1  $\mu$ M) in A549 cancer cells (Figure 18A). In contrast, it significantly enhances the effect in LNM35 cancer cells (Figure 18B). Similar results were also obtained when used in combination with higher concentration of Cisplatin (5  $\mu$ M) (Figure 18C, D). Additionally, 25 mM of DCA didn't enhances the anticancer effects of Camptothecin (0.01  $\mu$ M) and Gemcitabine (0.01  $\mu$ M) in both cell lines (Figure 18E, F, G, H).

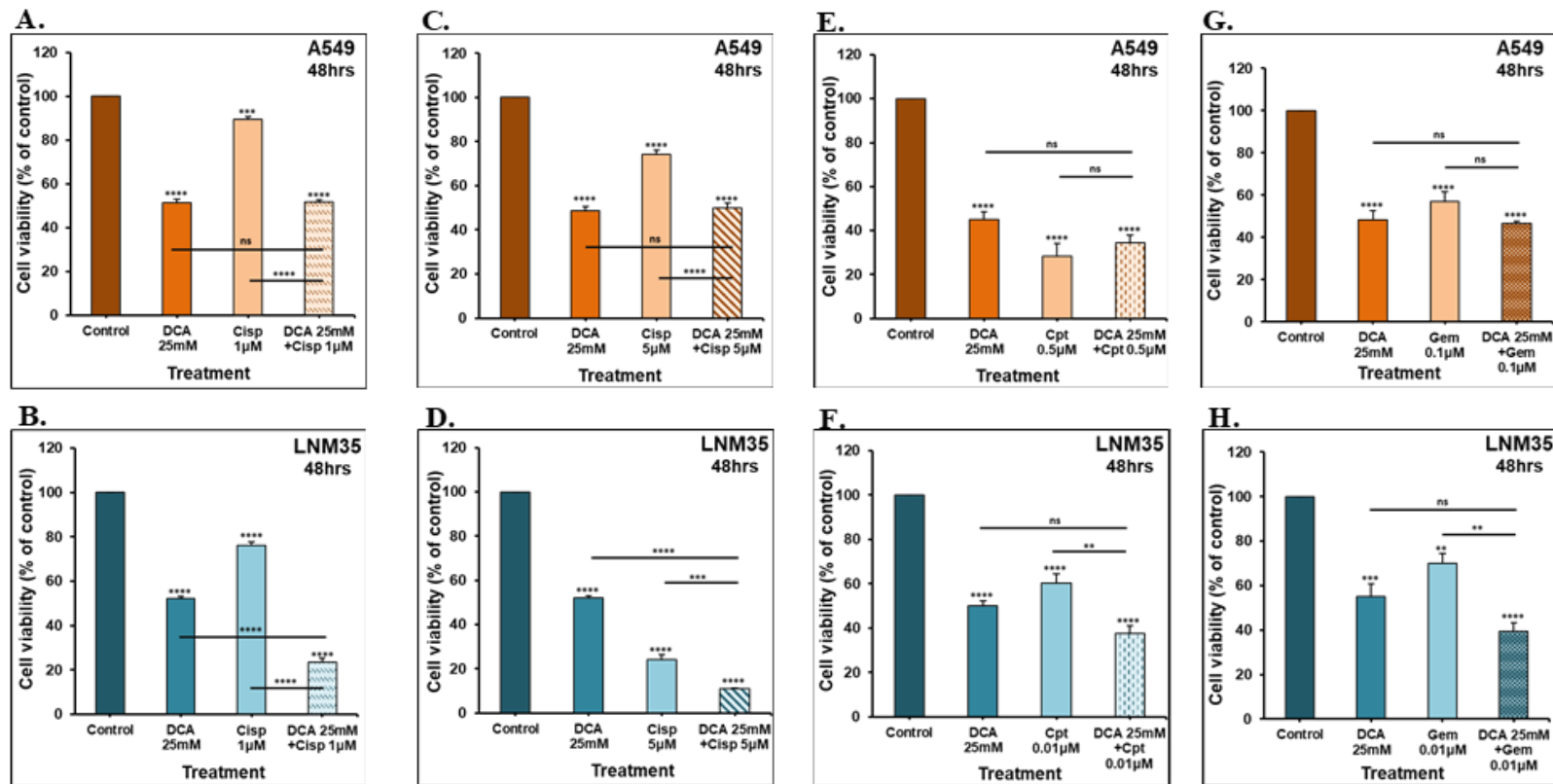


Figure 18: Effect of DCA in Combination with Chemotherapeutic Agents on the Viability of NSCLC Cells. Exponentially growing A549 cells (A, C) and LNM35 cells (B, D) were treated, in 96-well plate for 48 hrs, with DCA (25 mM) ± Cisplatin (1, 5 µM). Similarly, exponentially growing A549 cells were treated, in 96-well plate for 48 hrs, with DCA (25 mM) in combination with Camptothecin (0.5 µM) (E) or Gemcitabine (0.1 µM) (G) while LNM35 cells were treated with Camptothecin (0.01 µM) (F) or Gemcitabine (0.01 µM) (H). Cellular viability was determined using CellTiter Glo luminescent assay as described in the Material and Methods. Experiments were repeated at least 3 independent times. Columns represent means; bars represent S.E.M. \*\*Significantly different at <0.01. \*\*\*Significantly different at <0.001. \*\*\*\*Significantly different at <0.0001.

### **3.6 Effect of DCA in Combination with Frondoside A on NSCLC Cellular Viability and Colony Growth**

To further explore the anticancer spectrum of DCA, its effect on cellular viability and colony growth was investigated when combined with the natural triterpenoid glycoside, Frondoside A Hydrate. In the context of cellular viability, DCA (25 mM) significantly enhances the anticancer activity of Frondoside A (1  $\mu$ M) and (2.5  $\mu$ M) in A549 and LNM35 cancer cells, respectively (Figure 19A, B). On the other hand, 25 mM of DCA didn't significantly enhance the activity of Frondoside A in inhibiting the growth of pre-formed A549 and LNM35 colonies (Figure 19C, D, E).

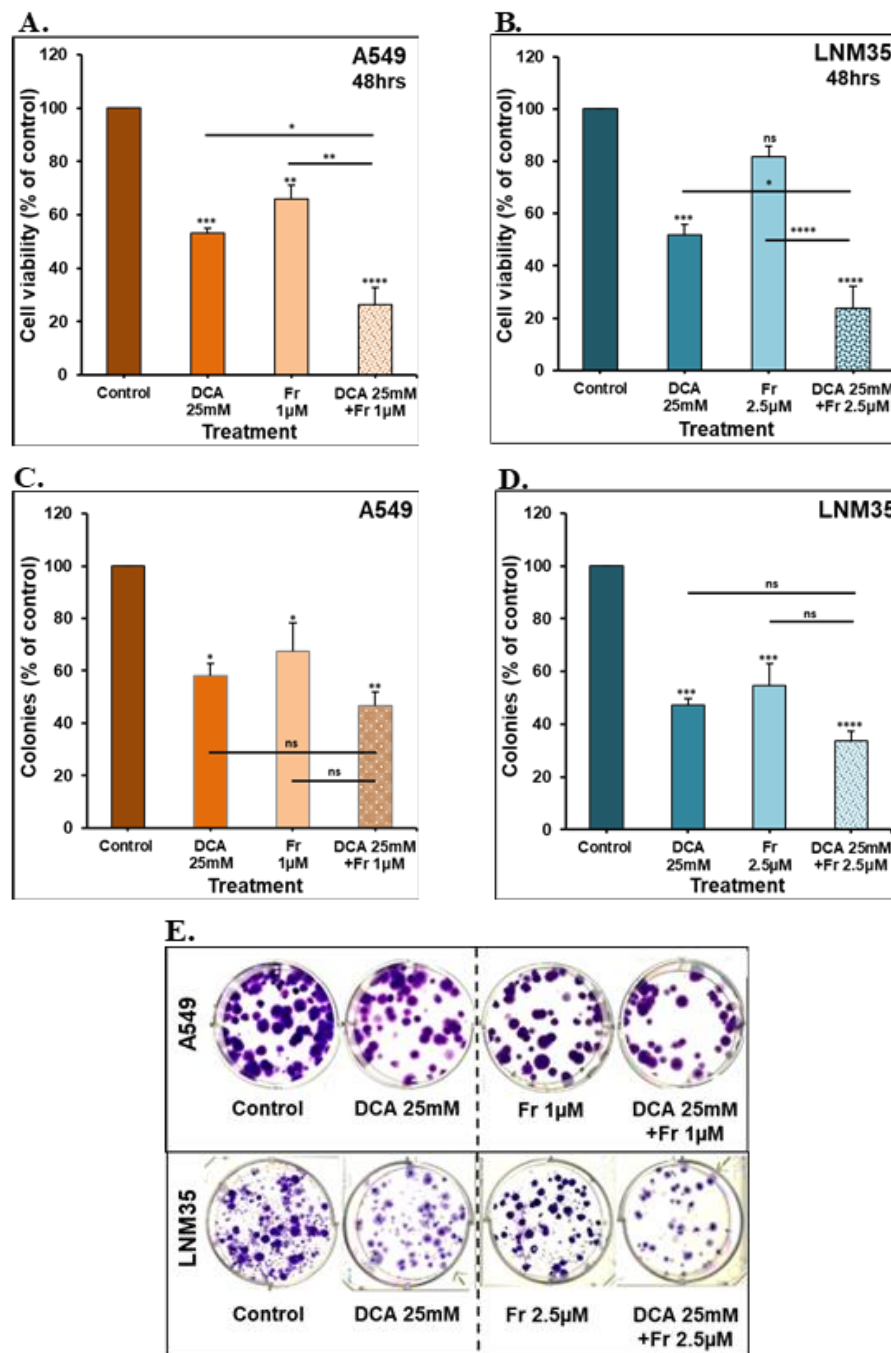


Figure 19: Effect of DCA in combination with Frondoside A on NSCLC Cells Viability and Colony Growth. (A, B) Exponentially growing A549 & LNM35 cancer cells were treated in 96-well plate for 48 hrs, with DCA (25 mM)  $\pm$  Frondoside A 1  $\mu$ M and 2.5  $\mu$ M, respectively. Cellular viability was determined as described in the Materials and Methods. A549 (C) and LNM35 (D) formed colonies were treated with the indicated concentrations, fixed, stained and counted as described in the Materials and Methods. (E) Representative pictures of the colonies for the control and combinations are shown for A549 and LNM35 cancer cells. All experiments were repeated for at least three independent times. Columns represent means; bars represent S.E.M. \*Significantly different at  $<0.05$ . \*\*Significantly different at  $<0.01$ . \*\*\*Significantly different at  $<0.001$ . \*\*\*\*Significantly different at  $<0.0001$ .

### **3.7 Effect of DCA in Combination with EGFR-TKi on NSCLC Cellular Viability and Colony Growth**

The impact of 48 hours incubation with increasing concentrations of Gefitinib and Erlotinib (5 - 80  $\mu$ M) was investigated on A549 and LNM35 cancer cells. Gefitinib caused a concentration dependent reduction in the viability of A549 and LNM35 cancer cells (Figure 20A, B); likewise, Erlotinib showed the same reduction pattern in the two cell lines (Figure 20C, D). 20  $\mu$ M of Gefitinib and Erlotinib has the ability in both cell lines to inhibit the cellular viability of A549 and LNM35 by approximately 40% and this concentration was used with DCA in the combination experiments.

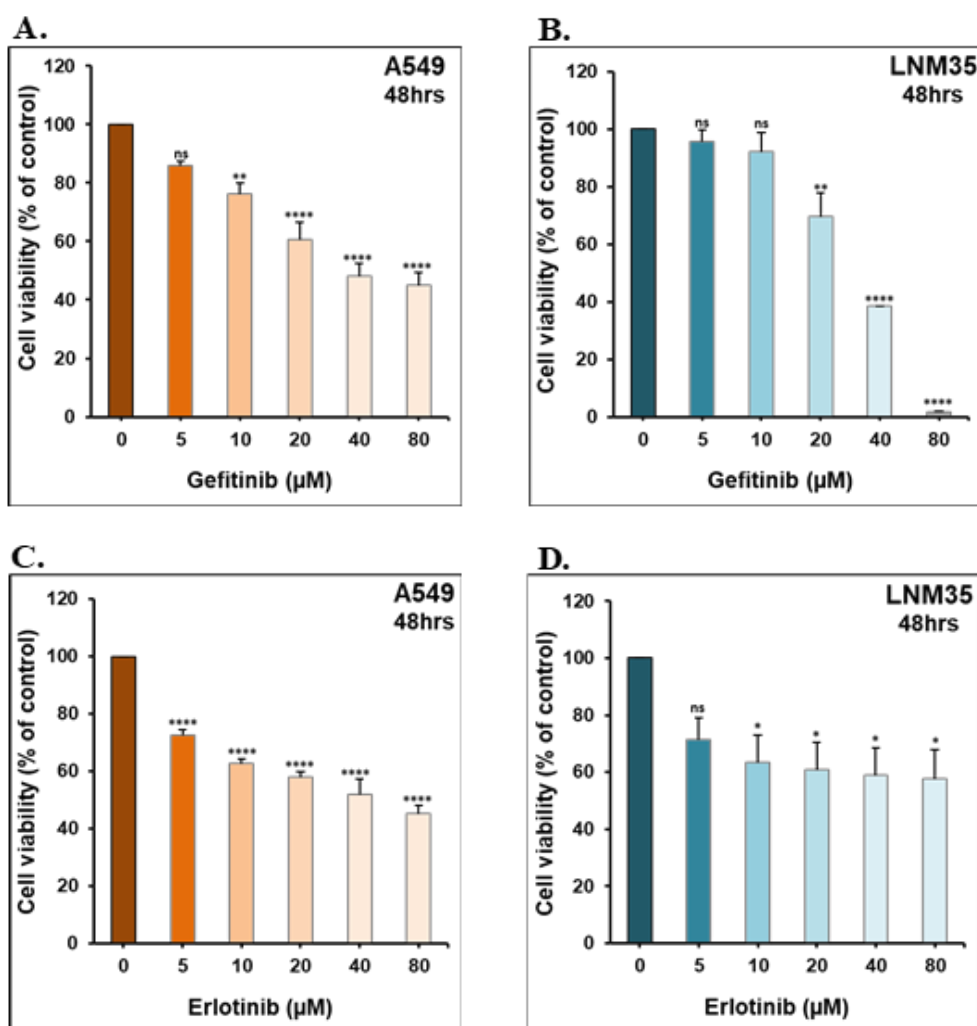


Figure 20: Effect of EGFR-Tki on NSCLC Cells Viability. Exponentially growing A549 (A, C) and LNM35 (B, D) cells were treated with drug vehicle, Gefitinib or Erlotinib (5 - 80 μM) for 48 hrs. Cellular viability was determined using CellTiter-Glo luminescent assay as described in the materials and methods. Experiments were repeated for at least 3 independent times. Columns are means; bars are S.E.M. ns non-significant. \*Significantly different at <0.05. \*\*Significantly different at <0.01. \*\*\*\*Significantly different at <0.0001.

Treatment of the cells for 48 hours with 25 mM of DCA significantly enhances the effect of Gefitinib on cellular viability of A549 (Figure 21A) and LNM35 (Figure 21B). Next, clonogenic assay was conducted to evaluate the effect of the combination on the growth of pre-formed colonies of both cell lines. 20 μM of Gefitinib caused 20-40% reduction in the percentage of total colonies in A549 (Figure 21C) and LNM35 (Figure 21D). Compared to the individual treatments, combination of DCA with

Gefitinib leads to a significant reduction in the percentage of total colonies of both cell lines (Figure 21C, D). In addition, this combination shows significant decrease in the cell density of the individual colonies of both cell lines (Figure 21E, F).

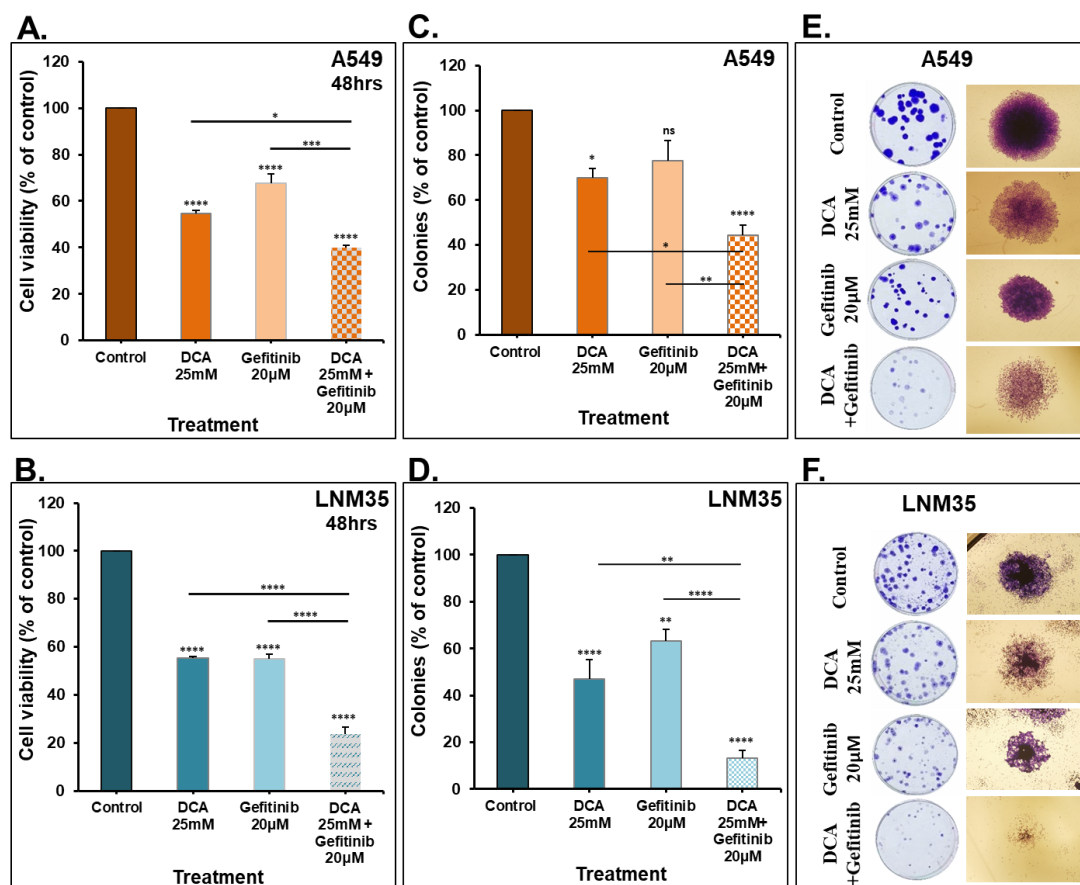


Figure 21: Effect of DCA in Combination with Gefitinib on NSCLC cells Viability and Colony Growth. Exponentially growing A549 (A) and LNM35 (B) cells were treated respectively, with DCA (25 mM)  $\pm$  Gefitinib 20  $\mu$ M. Cellular viability was determined using CellTiter-Glo luminescent assay. (C, D) Treatment of the pre-formed colonies of A549 and LNM35 cells, respectively with DCA (25 mM)  $\pm$  Gefitinib 20  $\mu$ M for 7 days after which colonies were fixed, stained and counted as described in the Materials and Methods. (E, F) Representative images of the colonies for the control and treated groups are shown for A549 and LNM35 cancer cells. All experiments were repeated for at least 3 independent times. Columns are means; bars are S.E.M. ns non-significant. \*Significantly different at  $<0.05$ . \*\*Significantly different at  $<0.01$ . \*\*\*Significantly different at  $<0.001$ . \*\*\*\*Significantly different at  $<0.0001$ .

Similarly, DCA enhances the inhibitory effect of Erlotinib on the cellular viability of A549 and LNM35 (Figure 22A, B). The percentage of A549 and LNM35 total colonies was significantly reduced with Erlotinib by 30-40% (Figure 22C, D) and

this reduction was enhanced by DCA in LNM35 (Figure 22D) and not A549 (Figure 22C). Despite of the non-significant reduction in the percentage of A549 colonies with the combination, the cell density of each colony was significantly reduced compared to the individual treatments (Figure 22E). Likewise, the cell density of the LNM35 colonies was reduced in the combination-treated group (Figure 22F).

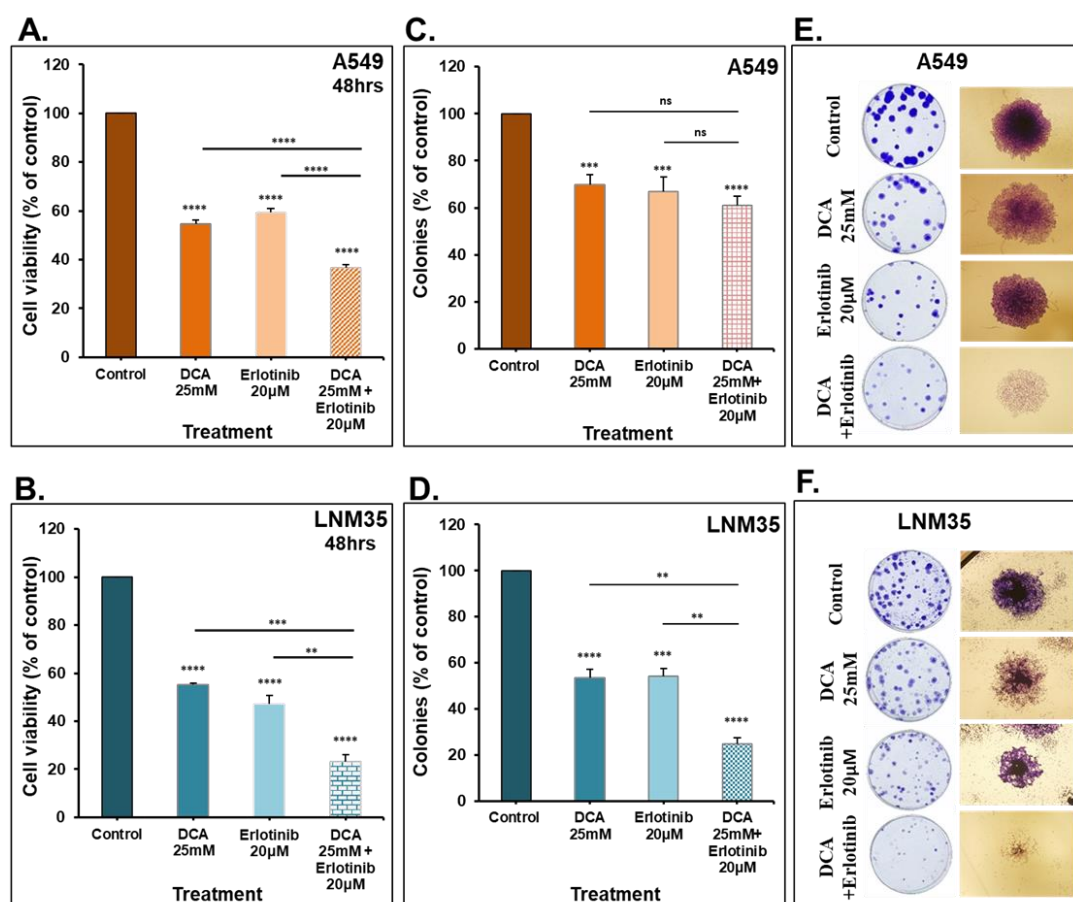


Figure 22: Effect of DCA in Combination with Erlotinib on NSCLC Cells Viability and Colony Growth. Exponentially growing A549 (A) and LNM35 (B) cells were treated respectively, with DCA (25 mM) ± Erlotinib 20 µM. Cellular viability was determined using CellTiter-Glo luminescent assay. (C, D) Treatment of the pre-formed colonies of A549 and LNM35 cells, respectively with DCA (25 mM) ± Erlotinib 20 µM for 7 days after which colonies were fixed, stained and counted as described in the Materials and Methods. (E, F) Representative images of the colonies for the control and treated groups are shown for A549 and LNM35 cancer cells. All experiments were repeated for at least 3 independent times. Columns are means; bars are S.E.M. ns non-significant. \*\*Significantly different at <0.01. \*\*\*Significantly different at <0.001. \*\*\*\*Significantly different at <0.0001.

## Chapter 4: Discussion

Despite of the recent great advances in the screening, diagnosis and management of lung cancer in addition to the remarkable progress in understanding the molecular biology, lung cancer is still considered a global burden by being the second most common cancer with the highest mortality rate worldwide in 2020 (WHO, 2020). Limitations of the classical chemotherapy in addition to the challenges surrounding the new evolutionary therapeutic agents in lung cancer could be the reasons behind such continuous burden. High cost, restricted efficacy to small therapeutically sensitive populations in addition to acquired resistance make inequalities between lung cancer patients in access such agents. Therefore, various efforts are being devoted to develop effective agents and strategies with good safety margin to target lung cancer in an attempt to provide cure or improve the patients outcomes. NSCLC is the most common histological subtype of lung cancer, accounting for approximately 85% of lung cancer cases. Metabolic remodeling is one of the emerging hallmarks of cancer including the major subtypes of NSCLC (Sellers et al., 2019). Evidence of metabolic alterations in the glucose, lipids and amino acids was reported recently in NSCLC cells which make such pathways a promising potential target to treat NSCLC (Mendes & Serpa, 2019). This study aims to investigate the impact of the metabolic drug DCA on lung cancer growth, migration, invasion and angiogenesis *in-vitro* and tumor growth and metastasis *in-vivo* in addition to investigate the effect of targeting metabolism by DCA on the cytotoxic effect of approved chemotherapy and targeted therapy as a step to achieve better efficacy with better safety margin.

Two lung cancer cell lines have been used namely, A549 and LNM35 cell lines. The former cell line resembles the ADC subtype of NSCLC which is considered as the most common type of NSCLC resembles approximately 40% of lung cancer. It arises from alveolar cells located in the smaller airway epithelium and tends to express TTF-1 and napsin A. The latter cell line represents LCC that accounts approximately for 5 to 10% of lung cancer. This type of NSCLC is typically poorly differentiated (Duma et al., 2019).

In the present study, the impact of DCA was investigated on the cellular viability and colony growth of NSCLC cell lines *in-vitro*. It was showed that DCA (3.125 - 100 mM) produced a concentration and time dependent reduction in the cellular viability and growth of pre-formed colonies of A549 and LNM35 cell lines. The IC<sub>50</sub> of DCA at 48 hours was approximately 25 mM in both cell lines. these results come in agreement with other reports in which DCA (10 - 90 mM) inhibited the cellular viability of colorectal cancer (CRC) cell lines namely, SW620, LS174t, LoVo and HT-29 in a dose dependent manner at 48 hours with IC<sub>50</sub> range 30 - 50 mM according to the cell line type (Liang et al., 2011). Similarly, DCA (20 mM) significantly decreased the viability of CRC cells namely, SW480, LoVo and HT-29 at 48 hours with greater effect on the poorly differentiated SW480 cells and metastatic LoVo cells compared to the well-differentiated HT-29 cells (Madhok et al., 2010). On the other hand, higher IC<sub>50</sub> was reported in cervical cancer cells Hela and SiHa cells (Li et al., 2017) while DCA (20 mM) failed to inhibit the cellular viability of breast cancer MCF-7 cell line (Woo et al., 2016).

These *in-vitro* data were validated by testing the effect of DCA on tumor progression *in-vivo* using chick embryo CAM and athymic mice models. Firstly, this

study demonstrated that a significant growth reduction was achieved in the A549 and LNM35 xenografted on chick embryo CAM by using DCA doses of 50 mM and 100 mM, respectively. This is the first study investigating the effect of DCA on NSCLC cells xenografted in chick embryo CAM. During the writing of this thesis, a study was published investigated the effect of sodium DCA on U87 MG and PBT24 glioblastoma cell lines xenografted on chick embryo CAM. The authors reported a variation in U87 MG and PBT24 tumor growth in response to the different concentrations of sodium DCA. It was reported that 10 mM of sodium DCA was effective in reducing the PBT24 tumor growth but not U87 tumor growth reflecting on some differences in the biology of the two cell lines (Stakišaitis et al., 2021). Secondly, considering the LD<sub>50</sub> of DCA in rats and mice are 4.5g/kg and 5.5g/kg, respectively (Anand et al., 2014; Laug, 2016), treatment with DCA at doses of 200 mg/kg everyday (5 days/week) caused a significant 40% reduction in xenografted A549 tumor growth while higher dose of DCA (500 mg/kg) was required to produce a significant reduction in xenografted LNM35 tumor growth. In this context, it has been previously reported that DCA (100 mg/kg) increased the tumor doubling time of A549 and H1975 NSCLC from approximately 3 to 6.5 days (Lu et al., 2018) but failed to produce a significant inhibitory effect in MDA-MB-231 tumor bearing mice (Robey & Martin, 2011). On the other hand, a significant growth delay was also observed in HT-29 xenografts treated with oral DCA (200 mg/kg) daily for four days (Lin et al., 2014).

Investigating the toxicity of the potential anticancer drugs is as important as investigating their efficacy since severe toxicity can comprise their use in the clinic. DCA showed no cytotoxicity to the chick embryos and athymic mice. The percentage of alive embryo was the same in DCA-treated and control groups. Additionally, DCA

didn't affect mice behavior, weight, complete blood count, liver and kidney function parameters compared to the control group. These findings are consistent with previously published preclinical and clinical reports that showed no evidence of severe hematologic, hepatic, renal, or cardiac toxicity with DCA treatment (Bonnet et al., 2007; Michelakis et al., 2010). Few patients, treated with DCA, complained from common gastrointestinal effects. Additionally, the most common limitation to DCA administration is reversible peripheral neuropathy which can be minimized by dose reduction or complementary administration of antioxidants (Tataranni & Piccoli, 2019). Incorporating DCA into drug delivery system (DDS) such as, nanoparticles, is a promising approach to retain the anticancer activity of DCA with minimal side effects (Abánades Lázaro, et al., 2018a; Abánades Lázaro, et al., 2018b; Abánades Lázaro, et al., 2018c).

The anticancer effect of DCA was reported to be partly due to induction of apoptosis as was observed in colorectal cancer cells (Madhok et al., 2010) and NSCLC cells (Lu et al., 2018) or due to inhibition of angiogenesis. Angiogenesis inhibitors such as the anti-VEGF antibody Bevacizumab and VEGF receptor blocker Ramucirumab have been approved clinically to treat lung cancer. Despite of their approved efficacy, their modest overall therapeutical effects with associated side effects of hypertension and increased stroke risk create a clear need for more effective approach targeting angiogenesis (Zirlik & Duyster, 2018). This study demonstrated that DCA (25 mM) is a promising anti-angiogenic agent by being able to significantly inhibit two essential steps in angiogenesis which are: endothelial cell tube formation and sprouting without inducing cytotoxicity. These findings are consistent with a previous report that showed a reduction in the tumor microvessel density in DCA-

treated rats in which HIF1 $\alpha$  suppression was also reported within the tumor cells (Sutendra et al., 2013). In addition, it was reported that 5 mM and 10 mM DCA inhibits HUVECs proliferation when low density cells (2000 cells/well) treated for 48 hours. In addition, these concentrations were reported to inhibit HUVECs migration *in-vitro* without affecting HUVECs tube formation when incubated for 4 hours (Schoonjans et al., 2020). On the other hand, Zhao and coworkers recently reported that DCA stimulates the angiogenesis in vascular dementia rats by improving the function of endothelial precursor cell (Zhao et al., 2019).

Approximately, 30-40% of NSCLC patients present with metastatic disease at the time of diagnosis. Distant metastases affect negatively on the treatment options, response and survival (Tamura et al., 2015) in addition for being the main cause of lung cancer deaths (Wu et al., 2021). Metastasis is a multistep process involving detachment of cancer cells, migration, invasion and colonization at distant sites. Therefore, therapeutic agents and regimens reducing such hallmark in cancer is of high importance in cancer therapy. Despite of demonstrated anti-angiogenic activity of DCA, this study showed no impact of DCA on the metastasis of LNM35 cells xenografted in athymic mice treated orally with an effective dose. In this study, LNM35 cells xenografted by subcutaneous inoculation in athymic mice produced a 90% incidence of axillary lymph node metastases and DCA failed to reduce the incidence and the growth of lymph node metastases. It was reported previously that LNM35 cell line is the first human lung cancer cell line with lymphogenous metastatic properties with 100% incidence following a subcutaneous inoculation (Kozaki et al., 2000). Additionally, DCA didn't show inhibitory effects on the migratory and invasive properties of LNM35 and A549 cells *in-vitro*. Similarly, it was reported that DCA

monotherapy was not effective in reducing lung metastases from metastatic breast cancer cells xenografted in nude mice (Robey & Martin, 2011).

Combination therapy has been a fundamental approach in cancer therapy. Combining different anticancer drugs allows the targeting of different essential signaling pathways to enhance the therapeutic benefits, avoid the acquired resistance and decrease the severity of side effects (Katzung et al., 2012). NSCLC stage, histology, genetic alteration and the patient's condition determine the best combination of treatment modalities. Chemotherapy plays an integral part in the management of NSCLC patients. A regimen of platinum (Cisplatin or Carboplatin) plus Paclitaxel, Gemcitabine, Docetaxel, Vinorelbine, Irinotecan, or Pemetrexed is usually used (Zappa & Mousa, 2016). The nonselective characteristics of chemotherapeutic agents results in modest increase in survival with significant toxicity to the patient (Burris, 2009). This underscores the need for better strategies to improve patients' outcomes with minimal side effects. In the present study, DCA failed to enhance the anticancer effect of Camptothecin, and Gemcitabine in both NSCLC cell lines. Additionally, DCA failed to significantly enhance the anticancer effects of Cisplatin in A549 cell line *in-vitro* but it enhanced the cytotoxic effect of Cisplatin in LNM35 cell line reflecting on the role of genetic background of cancer cells in determining the cell death pathway induced by the drugs. Kim et al. (2019) reported that A549 cells have lower rate of aerobic glycolysis compared to H460 cells due to differential expression in some metabolic enzymes. Aerobic glycolysis in cancer has been linked to chemoresistance and inhibition of related pathways has been suggested as a mechanism for overcoming such resistance. For instance, overexpression of PDK4 in high grade bladder cancer make the coadministration of DCA with Cisplatin cause a

dramatic reduction in tumor growth compared to DCA or Cisplatin alone (Woolbright et al., 2018). Similarly, administration of DCA with Paclitaxel was reported as a successful approach to overcome the Paclitaxel-resistant NSCLC cells due to PDK2 overexpression (Sun et al., 2017). Furthermore, Galgamuwa *et al.* (2016) stated that pre-treatment with DCA significantly attenuated the nephrotoxicity induced by Cisplatin in mice with retaining the cisplatin anticancer effects.

Interest in natural compounds, in cancer treatment, has been increased since decades because of the overall medical and economical limitations of current therapies. Frondoside A is triterpenoid glycoside isolated from the Atlantic cucumber, *Cucumaria frondose* which was previously demonstrated as a promising potent anti-cancer effects against NSCLC (Attoub et al., 2013). This study showed that DCA enhance the anticancer effect of Frondoside A in the context of cellular viability but didn't affect on the compound ability to inhibit colony growth. Increasing the treatment duration or optimizing the sequence of treatments can enhance the effect on the colony growth. It was reported that DCA showed promising anticancer effects when combined with some natural compounds such as: Curcumin (Kan et al., 2018) and Betulin derivatives (Mihoub et al., 2018).

Discovery of the targeted therapy has helped the physicians to tailor the treatment options for NSCLC patients. Many targeted drugs have been developed and become part of the first-line treatment of NSCLC, such as Gefitinib and Erlotinib which are considered as the first generation of EGFR-TKi (Herbst et al., 2018). Gefitinib and Erlotinib were approved more than 10 years ago for the treatment of chemotherapy-naive patients with advanced EGFR-mutant NSCLC as first-line treatment. They are also used as second-line therapy after chemotherapy failure

(Cataldo et al., 2011). Some reports showed that Erlotinib has a good efficacy in patients with EGFR-wild type NSCLC (Yang et al., 2017) and a maintenance dose can benefit these patients after platinum-based chemotherapy that considered the backbone therapy in wild-type EGFR NSCLC (Raimbourg et al., 2017). Despite of the remarkable benefits, many patients acquired therapeutic resistance after 10-14 months of treatment due to secondary mutation in EGFR gene (Yuan et al., 2019). Additionally, patients with some other mutations such as KRAS and PIK3CA showed primary resistance to the treatment of EGFR-TKi (Tetsu et al., 2016).

According to Cancer DepMap Portal, A549 cell line used in this study harbor wild-type EGFR and PIK3CA with mutant KRAS and NCI-H460 cell line, from which the LNM35 was derived, harbor wild-type EGFR with mutant PIK3CA and KRAS. In this study, the objective was to investigate the ability of DCA to sensitize the EGFR wild-type/KRAS mutant NSCLC cell lines when combined with Gefitinib or Erlotinib *in-vitro*. This study showed that DCA enhanced the inhibitory effect of Gefitinib on viability, colonies number and density in A549 and LNM35. Similarly, DCA enhances the effect of Erlotinib on the cellular viability of both cell lines. It also enhances the effect of Erlotinib on colonies number of LNM35 but not A549. Despite of this nonsignificant impact on the number of colonies, the density of individual colonies was significantly decreased with the combination in both A549 and LNM35. This observation also suggest that a longer duration treatment may be needed to achieve comparable decrease in A549 colonies number. To confirm that, an extra clonogenic experiment is ongoing in the lab to investigate the effect of longer duration treatment with combination on A549 cells. In this context, Yang and Tam (2016) reported that DCA with Gefitinib or Erlotinib synergistically inhibit the viability and colony

formation capacity of EGFR-mutant cells (NCI-H1975 and NCI-H1650) due to synergistic effect in promoting apoptosis. In EGFR wild-type cells (A549 and NCI-H460), they showed, in comparison to the individual treatments, that combination caused an elevated fraction affected (Fa) value in cellular viability without reaching level of synergism in EGFR wild-type cells (A549 and NCI-H460) and this combination didn't significantly repress the colony formation of these cell lines. The differences in the experimental conditions between the aforementioned report and this study could explain such variable results. In their clonogenic assay, the investigators treated the individual cells for 3 continuous days followed by incubation with drug-free medium for 15 days to form colonies however in this study experiments, the cells were firstly incubated to form colonies followed by treatment for 7 days. Furthermore, targeting KRAS signaling pathway was reported as a promising strategy in several studies to sensitize the KRAS mutant cells to EGFR-TKi (Chen et al., 2013; Park et al., 2010). The potential mechanism behind enhancing the response of the KRAS-mutant NSCLC cells to EGFR-TKi can be partly due to inhibition of PDK4 by DCA. Trinidad *et al.*, (2017) reported that PDK4 regulate the localization and activity of mutant KRAS and its tumorigenic properties suggesting PDK4 inhibition as a novel strategy to target KRAS mutant lung and colorectal cancers. Furthermore, autophagy inhibition was reported to facilitate the antitumor effects of EGFR-TKi (Han et al., 2011; Meng et al., 2019). In this context, DCA showed an ability to inhibit the autophagy by activating the AKT-mTOR pathway in NSCLC (Lu et al., 2018) which can be another possible mechanism behind enhancing the antitumor effects of EGFR-TKi.

The findings of this study pave the way for validating the impact of the combination of DCA with Gefitinib or Erlotinib on tumor growth *in-vivo* in addition to investigate the impact of DCA when combined with the second- and third generation EGFR-TKi. Other NSCLC cell lines harboring wild-type EGFR, KRAS and PIK3CA can be relevant models to determine if the wild status of these three genes will further increase the efficacy of the combination of DCA with EGFR-TKi.

## Chapter 5: Conclusion

In summary, this study demonstrated that DCA is a promising anticancer for NSCLC by being able to inhibit the cellular viability and colony growth of NSCLC cells *in-vitro* and tumor growth in the chick embryo CAM and nude mice in which the safety of this agent was also assessed. DCA inhibits the ability of endothelial cells to form capillary-like structures and sprouting *in-vitro* suggesting the inhibition of angiogenesis as a potential mechanism behind the anticancer effect. This study also revealed the potential value of DCA when combined with Gefitinib or Erlotinib *in-vitro*.

## References

- Abánades Lázaro, I., Abánades Lázaro, S., & Forgan, R. S. (2018a). Enhancing anticancer cytotoxicity through bimodal drug delivery from ultrasmall Zr MOF nanoparticles. *Chemical Communications*, 54(22), 2792-2795.
- Abánades Lázaro, I., Haddad, S., Rodrigo-Muñoz, J. M., Marshall, R. J., Sastre, B., Del Pozo, V., Fairen-Jimenez, D., & Forgan, R. S. (2018b). Surface-Functionalization of Zr-Fumarate MOF for Selective Cytotoxicity and Immune System Compatibility in Nanoscale Drug Delivery. *ACS Applied Materials and Interfaces*, 10(37), 31146-31157.
- Abánades Lázaro, I., Haddad, S., Rodrigo-Muñoz, J. M., Orellana-Tavra, C., Del Pozo, V., Fairen-Jimenez, D., & Forgan, R. S. (2018c). Mechanistic Investigation into the Selective Anticancer Cytotoxicity and Immune System Response of Surface-Functionalized, Dichloroacetate-Loaded, UiO-66 Nanoparticles. *ACS Applied Materials and Interfaces*, 10(6), 5255-5268.
- Alexander, M., Kim, S. Y., & Cheng, H. (2020). Update 2020: Management of Non-Small Cell Lung Cancer. *Lung*, 198(6), 897-907.
- Alkhazraji, A., Elgamal, M., Ang, S. H., & Shivarov, V. (2019). All cancer hallmarks lead to diversity. *Int J Clin Exp Med*, 12(1), 132-157.
- American Cancer Society. (2016). Lung Cancer ( Non-Small Cell ) What is non-small cell lung cancer ?, *American Cancer Society*, (Access Date 30/06/2021).
- American Cancer Society. (2019). Lung Cancer Early Detection, Diagnosis, and Staging. *New York, NY: Springer* (Access Date 30/06/2019).
- Amin, M. B., Greene, F. L., Edge, S. B., Compton, C. C., Gershenwald, J. E., Brookland, R. K., Meyer, L., Gress, D. M., Byrd, D. R., Winchester D. P., (2017). The Eighth Edition AJCC Cancer Staging Manual: Continuing to build a bridge from a population-based to a more "personalized" approach to cancer staging. *Cancer Journal for Clinicians*, 67(2), 93-99.
- Anand, S. S., Philip, B. K., & Mehendale, H. M. (2014). Chlorination Byproducts. In Philip Wexler (Ed.), *Encyclopedia of Toxicology: Third Edition*, Waltham, MA: Academic Press.
- Attoub, S., Arafat, K., Gélaude, A., Sultan, M. A. Al, Bracke, M., Collin, P., Takahashi, T., Adrian, T. E., & Wever, O. De. (2013). Frondoside A Suppressive Effects on Lung Cancer Survival, Tumor Growth, Angiogenesis, Invasion, and Metastasis. *PLOS ONE*, 8(1), e53087. <https://doi.org/10.1371/journal.pone.0053087>.

- Bonnet, S., Archer, S. L., Allalunis-Turner, J., Haromy, A., Beaulieu, C., Thompson, R., Lee, C. T., Lopaschuk, G. D., Puttagunta, L., Bonnet, S., Harry, G., Hashimoto, K., Porter, C. J., Andrade, M. A., Thebaud, B., & Michelakis, E. D. (2007). A Mitochondria-K<sup>+</sup> Channel Axis Is Suppressed in Cancer and Its Normalization Promotes Apoptosis and Inhibits Cancer Growth. *Cancer Cell*, 11(1), 37-51.
- Burris, H. A. (2009). Shortcomings of current therapies for non-small-cell lung cancer: unmet medical needs. *Oncogene*, 28, 4-13.
- Carmeliet, P. (2003). Angiogenesis in health and disease. In *Nature Medicine*, 9, 653-660.
- Cascone, V., Tomaino, A., Florio, P., Cristani, M., & Rizza, G. (2013). TCH-015 Evaluation of the Chemical and Physical Stability of Sodium Dichloroacetate, an Orphan Drug For Rare Metabolic Diseases. *European Journal of Hospital Pharmacy*, 20(1), A74. <http://dx.doi.org/10.1136/ejhpharm-2013-000276.206>.
- Cataldo, V. D., Gibbons, D. L., Pérez-Soler, R., & Quintás-Cardama, A. (2011). Treatment of Non-Small-Cell Lung Cancer with Erlotinib or Gefitinib. *New England Journal of Medicine*, 364(10), 947-955.
- Chen, J., Bi, H., Hou, J., Zhang, X., Zhang, C., Yue, L., Wen, X., Liu, D., Shi, H., Yuan, J., Liu, J., & Liu, B. (2013). Atorvastatin overcomes gefitinib resistance in KRAS mutant human non-small cell lung carcinoma cells. *Cell Death & Disease*, 4(9), e814. <https://doi.org/10.1038/cddis.2013.312>.
- Chiang, S. P. H., Cabrera, R. M., & Segall, J. E. (2016). Tumor cell intravasation. *American Journal of Physiology - Cell Physiology*, 311(1), C1-C14.
- Costa, F., & Soares, R. (2009). Nicotine: A pro-angiogenic factor. In *Life Sciences*, 84(23-24), 785-790.
- de Groot, P. M., Wu, C. C., Carter, B. W., & Munden, R. F. (2018). The epidemiology of lung cancer. In *Translational Lung Cancer Research*. 7(3), 220-233.
- Dejana, E., Orsenigo, F., Molendini, C., Baluk, P., & McDonald, D. M. (2009). Organization and signaling of endothelial cell-to-cell junctions in various regions of the blood and lymphatic vascular trees. In *Cell and Tissue Research*. 335(1), 17-25.
- Dela Cruz, C. S., Tanoue, L. T., & Matthay, R. A. (2011). Lung Cancer: Epidemiology, Etiology, and Prevention. In *Clinics in Chest Medicine*. 32(4), 605-44.
- Detterbeck, F. C. (2018). The eighth edition TNM stage classification for lung cancer: What does it mean on main street?. In *Journal of Thoracic and Cardiovascular Surgery*. 155(1), 356-359.

- Duma, N., Santana-Davila, R., & Molina, J. R. (2019). Non–Small Cell Lung Cancer: Epidemiology, Screening, Diagnosis, and Treatment. *Mayo Clinic Proceedings*, 94(8), 1623-1640.
- El-Metwally, T. H. (2009). *Cancer biology: An updated global overview (30-45)*. First edition. New York: Nova Science.
- Faubert, B., Solmonson, A., & DeBerardinis, R. J. (2020). Metabolic reprogramming and cancer progression. In *Science*. 368(6487), eaaw5473. <https://doi.org/10.1126/science.aaw5473>.
- Fernando, N. T., Koch, M., Rothrock, C., Gollogly, L. K., D'Amore, P. A., Ryeom, S., & Yoon, S. S. (2008). Tumor escape from endogenous, extracellular matrix-associated angiogenesis inhibitors by up-regulation of multiple proangiogenic factors. *Clinical Cancer Research*. 14(5), 1529-39.
- Fouad, Y. A., & Aanei, C. (2017). Revisiting the hallmarks of cancer. In *American Journal of Cancer Research*, 7(5), 1016-1036.
- Galgamuwa, R., Hardy, K., Dahlstrom, J. E., Blackburn, A. C., Wium, E., Rooke, M., Cappello, J. Y., Tummala, P., Patel, H. R., Chuah, A., Tian, L., McMorrow, L., Board, P. G., & Theodoratos, A. (2016). Dichloroacetate Prevents Cisplatin-Induced Nephrotoxicity without Compromising Cisplatin Anticancer Properties. *Journal of the American Society of Nephrology*, 27(11), 3331-3344.
- Gerhardt, H., Golding, M., Fruttiger, M., Ruhrberg, C., Lundkvist, A., Abramsson, A., Jeltsch, M., Mitchell, C., Alitalo, K., Shima, D., & Betsholtz, C. (2003). VEGF guides angiogenic sprouting utilizing endothelial tip cell filopodia. *Journal of Cell Biology*, 161(6), 1163-1177.
- Garon, E. B., Christofk, H. R., Hosmer, W., Britten, C. D., Bahng, A., Crabtree, M. J., Hong, C. S., Kamranpour, N., Pitts, S., Kabbinavar, F., Patel, C., Von Euw, E., Black, A., Michelakis, E. D., Dubinett, S. M., & Slamon, D. J. (2014). Dichloroacetate should be considered with platinum-based chemotherapy in hypoxic tumors rather than as a single agent in advanced non-small cell lung cancer. *Journal of Cancer Research and Clinical Oncology*, 140(3). 443-452.
- Hadler-Olsen, E., Winberg, J. O., & Uhlin-Hansen, L. (2013). Matrix metalloproteinases in cancer: Their value as diagnostic and prognostic markers and therapeutic targets. In *Tumor Biology*, 34(4), 2041-51.
- Hall, K., & Ran, S. (2010). Regulation of tumor angiogenesis by the local environment. *Frontiers in Bioscience*, 15, 195-212.
- Han, W., Pan, H., Chen, Y., Sun, J., Wang, Y., Li, J., Ge, W., Feng, L., Lin, X., Wang, X., Wang, X., & Jin, H. (2011). EGFR Tyrosine Kinase Inhibitors Activate Autophagy as a Cytoprotective Response in Human Lung Cancer Cells. *PLoS ONE*, 6(6), e18691. <https://doi.org/10.1371/journal.pone.0018691>.

- Hapach, L. A., Mosier, J. A., Wang, W., & Reinhart-King, C. A. (2019). Engineered models to parse apart the metastatic cascade. *Npj Precision Oncology*, 3, 20. <https://doi.org/10.1038/s41698-019-0092-3>.
- Harris, T. J. C., & Tepass, U. (2010). Adherens junctions: From molecules to morphogenesis. In *Nature Reviews Molecular Cell Biology*, 11, 502-514.
- Hecht, S. S. (2012). Lung carcinogenesis by tobacco smoke. *International Journal of Cancer*, 131(12), 2724-2732.
- Herbst, R. S., Morgensztern, D., & Boshoff, C. (2018). The biology and management of non-small cell lung cancer. In *Nature*, 553(7689), 446-454.
- Hida, K., Maishi, N., Torii, C., & Hida, Y. (2016). Tumor angiogenesis—characteristics of tumor endothelial cells. In *International Journal of Clinical Oncology*, 21(2), 206-212.
- Houlihan, N. G., & Tyson, L. B. (2012). *Lung Cancer*. Second edition, Pittsburgh: Oncology Nursing Society.
- IARC-WHO. (2020). GLOBOCAN. In *GLOBOCAN 2020*. <https://gco.iarc.fr/> (Access Date 25/06/2021)
- Park I., Kim J. Y., Jung J., Han J. (2010). Lovastatin overcomes gefitinib resistance in human non-small cell lung cancer cells with K-Ras mutations. *Investigational New Drugs*, 28(6), 791-799.
- James, M. O., Jahn, S. C., Zhong, G., Smeltz, M. G., Hu, Z., & Stacpoole, P. W. (2017). Therapeutic applications of dichloroacetate and the role of glutathione transferase zeta-1. In *Pharmacology and Therapeutics*, 170, 166-180.
- Janning, M., & Loges, S. (2018). Anti-Angiogenics: Their Value in Lung Cancer Therapy. In *Oncology Research and Treatment*, 41(4), 172-180.
- Kalluri, R., & Weinberg, R. A. (2009). The basics of epithelial-mesenchymal transition. In *Journal of Clinical Investigation*, 119(6), 1420-8.
- Kan, P. C., Chang, Y. J., Chien, C. S., Su, C. Y., & Fang, H. W. (2018). Coupling dichloroacetate treatment with curcumin significantly enhances anticancer potential. *Anticancer Research*, 38(11), 6253-6261.
- Kankotia, S., & Stacpoole, P. W. (2014). Dichloroacetate and cancer: New home for an orphan drug? In *Biochimica et Biophysica Acta - Reviews on Cancer*, 1846(2), 617-29.
- Katzung, B. G., Masters, S. B., & Trevor, A. J. (2012). *Basic & Clinical Pharmacology*. Twelfth edition. US: McGraw Hill.

- Kim, S., Jang, J.-Y., Koh, J., Kwon, D., Kim, Y. A., Paeng, J. C., Ock, C.-Y., Keam, B., Kim, M., Kim, T. M., Heo, D. S., Chung, D. H., & Jeon, Y. K. (2019). Programmed cell death ligand-1-mediated enhancement of hexokinase 2 expression is inversely related to T-cell effector gene expression in non-small-cell lung cancer. *Journal of Experimental & Clinical Cancer Research*, 38(1), 462. <https://doi.org/10.1186/s13046-019-1407-5>.
- Kozaki, K. I., Miyaishi, O., Tsukamoto, T., Tatematsu, Y., Hida, T., Takahashi, T., & Takahashi, T. (2000). Establishment and characterization of a human lung cancer cell line NCI- H460-LNM35 with consistent lymphogenous metastasis via both subcutaneous and orthotopic propagation. *Cancer Research*, 60(9), 2535-2540.
- Kumar, A., Kant, S., & Singh, S. M. (2012). Novel molecular mechanisms of antitumor action of dichloroacetate against T cell lymphoma: Implication of altered glucose metabolism, pH homeostasis and cell survival regulation. *Chemico-Biological Interactions*, 199(1), 29-37.
- Laug, E. P. (2016). Effect of Acetic, Monochloroacetic, Dichloroacetic, and Trichloroacetic Acids on Oxygen Consumption of Mouse Liver: *Proceedings of the society for experimental biology and medicine*, 61(2), 178-179.
- Lemjabbar-Alaoui, H., Hassan, O. U. I., Yang, Y. W., & Buchanan, P. (2015). Lung cancer: Biology and treatment options. In *Biochimica et Biophysica Acta - Reviews on Cancer*, 1856(2), 189-210.
- Levine, A. J., & Puzio-Kuter, A. M. (2010). The control of the metabolic switch in cancers by oncogenes and tumor suppressor genes. In *Science*, 330(6009), 1340-4.
- Li, B., Li, X., Xiong, H., Zhou, P., Ni, Z., Yang, T., Zhang, Y., Zeng, Y., He, J., Yang, F., Zhang, N., Wang, Y., Zheng, Y., & He, F. (2017). Inhibition of COX2 enhances the chemosensitivity of dichloroacetate in cervical cancer cells. *Oncotarget*, 8(31), 51748-51757.
- Liang, H., Tong, J., Xie, G., He, J., Li, J., & Pan, F. (2011). Synergistic antitumor effect of dichloroacetate in combination with 5-fluorouracil in colorectal cancer. *Journal of Biomedicine and Biotechnology*, 2011, 740564. <https://doi.org/10.1155/2011/740564>.
- Lin, G., Hill, D. K., Andrejeva, G., Boulton, J. K. R., Troy, H., Fong, A. C. L. F. W. T., Orton, M. R., Panek, R., Parkes, H. G., Jafar, M., Koh, D. M., Robinson, S. P., Judson, I. R., Griffiths, J. R., Leach, M. O., Eykyn, T. R., & Chung, Y. L. (2014). Dichloroacetate induces autophagy in colorectal cancer cells and tumours. *British Journal of Cancer*, 111(2), 375-85.
- Lu, T., Yang, X., Huang, Y., Zhao, M., Li, M., Ma, K., Yin, J., Zhan, C., & Wang, Q. (2019). Trends in the incidence, treatment, and survival of patients with lung cancer in the last four decades. *Cancer Management and Research*, 11, 943-953.

- Lu, X., Zhou, D., Hou, B., Liu, Q. X., Chen, Q., Deng, X. F., Yu, Z. Bin, Dai, J. G., & Zheng, H. (2018). Dichloroacetate enhances the antitumor efficacy of chemotherapeutic agents via inhibiting autophagy in non-small-cell lung cancer. *Cancer Management and Research*, *10*, 1231-1241.
- Lugano, R., Ramachandran, M., & Dimberg, A. (2020). Tumor angiogenesis: causes, consequences, challenges and opportunities. In *Cellular and Molecular Life Sciences*, *77*(9), 1745-1770.
- Madhok, B. M., Yeluri, S., Perry, S. L., Hughes, T. A., & Jayne, D. G. (2010). Dichloroacetate induces apoptosis and cell-cycle arrest in colorectal cancer cells. *British Journal of Cancer*, *102*(12), 1746-52.
- Malarkey, D. E., Hoenerhoff, M., & Maronpot, R. R. (2013). Carcinogenesis: Mechanisms and Manifestations, Haschek and Rousseaux's handbook of toxicologic pathology (107-146). Waltham, MA: Academic Press.
- Manzo, A., Montanino, A., Carillio, G., Costanzo, R., Sandomenico, C., Normanno, N., Piccirillo, M. C., Daniele, G., Perrone, F., Rocco, G., & Morabito, A. (2017). Angiogenesis inhibitors in NSCLC. In *International Journal of Molecular Sciences*, *18*(10), 2021. <https://doi.org/10.3390/ijms18102021>.
- Meirson, T., Gil-Henn, H., & Samson, A. O. (2020). Invasion and metastasis: the elusive hallmark of cancer. In *Oncogene*, *39*(9), 2024-2026.
- Mendes, C., & Serpa, J. (2019). Metabolic remodelling: An accomplice for new therapeutic strategies to fight lung cancer. In *Antioxidants*, *8*(12), 603. <https://doi.org/10.3390/antiox8120603>.
- Meng, J., Chang, C., Chen, Y., Bi, F., Ji, C., & Liu, W. (2019). EGCG overcomes gefitinib resistance by inhibiting autophagy and augmenting cell death through targeting ERK phosphorylation in NSCLC. *OncoTargets and Therapy*, *12*, 6033-6043.
- Mezquita, P., Parghi, S. S., Brandvold, K. A., & Ruddell, A. (2005). Myc regulates VEGF production in B cells by stimulating initiation of VEGF mRNA translation. *Oncogene*, *24*, 889-901.
- Michelakis, E. D., Sutendra, G., Dromparis, P., Webster, L., Haromy, A., Niven, E., Maguire, C., Gammer, T. L., Mackey, J. R., Fulton, D., Abdulkarim, B., McMurtry, M. S., & Petruk, K. C. (2010). Metabolic modulation of glioblastoma with dichloroacetate. *Science Translational Medicine*, *2*(31), 31ra34. <https://doi.org/10.1126/scitranslmed.3000677>.
- Michelakis, E. D., Webster, L., & Mackey, J. R. (2008). Dichloroacetate (DCA) as a potential metabolic-targeting therapy for cancer. In *British Journal of Cancer*, *99*(7), 989-994.

- Mihoub, M., Pichette, A., Sylla, B., Gauthier, C., & Legault, J. (2018). Bidesmosidic betulin saponin bearing L-rhamnopyranoside moieties induces apoptosis and inhibition of lung cancer cells growth in vitro and in vivo. *PLoS ONE*, *13*(3), e0193386. <https://doi.org/10.1371/journal.pone.0193386>.
- National Cancer Institute. (2018). *Types of Lung Cancer | SEER Training*. <https://training.seer.cancer.gov/lung/intro/types.html> (Access Date 30/06/2021).
- National Cancer Institute. (2020). *Cancer Classification | SEER Training Modules*. <https://training.seer.cancer.gov/disease/categories/classification.html> (Access Date 30/06/2021).
- Nishida, N., Yano, H., Nishida, T., Kamura, T., & Kojiro, M. (2006). Angiogenesis in cancer. In *Vascular Health and Risk Management*, *2*(3), 213-9
- Parker, M. S., Groves, R. C., & Kusmirek, J. E. (2017). *Lung Cancer Screening*. First edition. Thieme Medical Publishers.
- Perlikos, F., Harrington, K. J., & Syrigos, K. N. (2013). Key molecular mechanisms in lung cancer invasion and metastasis: A comprehensive review. In *Critical Reviews in Oncology/Hematology*, *87*(1), 1-11.
- Raimbourg, J., Joalland, M.-P., Cabart, M., Plater, L. de, Bouquet, F., Savina, A., Decaudin, D., Bennouna, J., Vallette, F. M., & Laliere, L. (2017). Sensitization of EGFR Wild-Type Non-Small Cell Lung Cancer Cells to EGFR-Tyrosine Kinase Inhibitor Erlotinib. *Molecular Cancer Therapeutics*, *16*(8), 1634-1644.
- Ribatti, D., Annese, T., Ruggieri, S., Tamma, R., & Crivellato, E. (2019). Limitations of Anti-Angiogenic Treatment of Tumors. In *Translational Oncology*, *12*(7), 981-986.
- Robey, I. F., & Martin, N. K. (2011). Bicarbonate and dichloroacetate: Evaluating pH altering therapies in a mouse model for metastatic breast cancer. *BMC Cancer*, *11*, 235.
- Saman, H., Raza, S. S., Uddin, S., & Rasul, K. (2020). Inducing angiogenesis, a key step in cancer vascularization, and treatment approaches. In *Cancers*, *12*(5), 1172. <https://doi.org/10.3390/cancers12051172>.
- Schoonjans, C. A., Mathieu, B., Joudiou, N., Zampieri, L. X., Brusa, D., Sonveaux, P., Feron, O., & Gallez, B. (2020). Targeting Endothelial Cell Metabolism by Inhibition of Pyruvate Dehydrogenase Kinase and Glutaminase-1. *Journal of Clinical Medicine*, *9*(10), 3308. <https://doi.org/10.3390/jcm9103308>.
- Sellers, K., Allen, T. D., Bousamra, M., Tan, J. L., Méndez-Lucas, A., Lin, W., Bah, N., Chernyavskaya, Y., MacRae, J. I., Higashi, R. M., Lane, A. N., Fan, T. W. M., & Yuneva, M. O. (2019). Metabolic reprogramming and Notch activity distinguish between non-small cell lung cancer subtypes. *British Journal of Cancer*, *121*(1), 51-64.

- Semenza, G. L. (2013). HIF-1 mediates metabolic responses to intratumoral hypoxia and oncogenic mutations. In *Journal of Clinical Investigation*, 123(9), 3664-71.
- Shi, Q., Le, X., Wang, B., Abbruzzese, J. L., Xiong, Q., He, Y., & Xie, K. (2001). Regulation of vascular endothelial growth factor expression by acidosis in human cancer cells. *Oncogene*, 20(28), 3751-6.
- Stacpoole, P. W. (2017). Therapeutic Targeting of the Pyruvate Dehydrogenase Complex/Pyruvate Dehydrogenase Kinase (PDC/PDK) Axis in Cancer. In *Journal of the National Cancer Institute*, 109(11), djx071. <https://doi.org/10.1093/jnci/djx071>
- Stakišaitis, D., Damanskienė, E., Curkūnavičiūtė, R., Juknevičienė, M., Alonso, M. M., Valančiūtė, A., Ročka, S., & Balnytė, I. (2021). The Effectiveness of Dichloroacetate on Human Glioblastoma Xenograft Growth Depends on Na<sup>+</sup> and Mg<sup>2+</sup> Cations. *Dose-Response*, 19(1), 1-14.
- Sun, H., Zhu, A., Zhou, X., & Wang, F. (2017). Suppression of pyruvate dehydrogenase kinase-2 re-sensitizes paclitaxel-resistant human lung cancer cells to paclitaxel. *Oncotarget*, 8(32), 52642-52650.
- Sun, R. C., Fadia, M., Dahlstrom, J. E., Parish, C. R., Board, P. G., & Blackburn, A. C. (2010). Reversal of the glycolytic phenotype by dichloroacetate inhibits metastatic breast cancer cell growth in vitro and in vivo. *Breast Cancer Research and Treatment*, 120(1), 253-60.
- Sun, W., Zhou, S., Chang, S. S., McFate, T., Verma, A., & Califano, J. A. (2009). Mitochondrial mutations contribute to HIF1 $\alpha$  accumulation via increased reactive oxygen species and up-regulated pyruvate dehydrogenase kinase 2 in head and neck squamous cell carcinoma. *Clinical Cancer Research*, 15(2), 476-84.
- Sutendra, G., Dromparis, P., Kinnaird, A., Stenson, T. H., Haromy, A., Parker, J. M. R., Mcmurtry, M. S., & Michelakis, E. D. (2013). Mitochondrial activation by inhibition of PDKII suppresses HIF1 $\alpha$  signaling and angiogenesis in cancer. *Oncogene*, 32(13), 1638-1650.
- Tamura, T., Kurishima, K., Nakazawa, K., Kagohashi, K., Ishikawa, H., Satoh, H., & Hizawa, N. (2015). Specific organ metastases and survival in metastatic non-small-cell lung cancer. *Molecular and Clinical Oncology*, 3(1), 217-221.
- Tan, W., & Huq, S. (2021). *Non-Small Cell Lung Cancer (NSCLC)*. <https://emedicine.medscape.com/article/279960-overview> (Access Date 20/06/2021)
- Tataranni, T., & Piccoli, C. (2019). Dichloroacetate (DCA) and Cancer: An Overview towards Clinical Applications. In *Oxidative Medicine and Cellular Longevity*, 2019, 8201079. <https://doi.org/10.1155/2019/8201079>.

- Tetsu, O., Hangauer, M. J., Phuchareon, J., Eisele, D. W., & McCormick, F. (2016). Drug Resistance to EGFR Inhibitors in Lung Cancer. *Chemotherapy*, *61*(5), 223-235.
- Tetzlaff, F., & Fischer, A. (2018). Human Endothelial Cell Spheroid-based Sprouting Angiogenesis Assay in Collagen. *BIO-PROTOCOL*, *8*(17), e2995. <https://doi.org/10.21769/BioProtoc.2995>.
- Tian, W., Cao, C., Shu, L., & Wu, F. (2020). Anti-angiogenic therapy in the treatment of non-small cell lung cancer. In *OncoTargets and Therapy*, *13*, 12113-12129.
- Tocris Bioscience. (2019). Researching Angiogenesis in Cancer. *News-Medical*. <https://www.news-medical.net/whitepaper/20190318/Researching-Angiogenesis-in-Cancer.aspx> (Access Date 25/06/2021)
- Tonini, T., Rossi, F., & Claudio, P. P. (2003). Molecular basis of angiogenesis and cancer, *22*, 6549-6556.
- Trinidad, A. G., Whalley, N., Rowlinson, R., Delpuech, O., Dudley, P., Rooney, C., & Critchlow, S. E. (2017). Pyruvate dehydrogenase kinase 4 exhibits a novel role in the activation of mutant KRAS, regulating cell growth in lung and colorectal tumour cells. *Oncogene*, *36*(44), 6164-6176.
- Van Zijl, F., Krupitza, G., & Mikulits, W. (2011). Initial steps of metastasis: Cell invasion and endothelial transmigration. In *Mutation Research - Reviews in Mutation Research*, *728*(1-2), 23-34.
- Vaupel, P., & Multhoff, G. (2021). Revisiting the Warburg effect: historical dogma versus current understanding. In *Journal of Physiology*, *599*(6), 1745-1757.
- Vaupel, P., Schmidberger, H., & Mayer, A. (2019). The Warburg effect: essential part of metabolic reprogramming and central contributor to cancer progression. In *International Journal of Radiation Biology*, *95*(7), 912-919.
- Wang, S., & Olson, E. N. (2009). Angiomirs-Key regulators of angiogenesis. In *Current Opinion in Genetics and Development*, *19*(3), 205-11.
- Wang, W., Lollis, E. M., Bordeleau, F., & Reinhart-King, C. A. (2019). Matrix stiffness regulates vascular integrity through focal adhesion kinase activity, *33*(1), 1199-1208.
- WHO. (2020). *Who Report on Cancer*. <https://apps.who.int/iris/handle/10665/330745> (Access Date 20/06/2021).
- Woo, S. H., Seo, S. K., Park, Y., Kim, E. K., Seong, M. K., Kim, H. A., Song, J. Y., Hwang, S. G., Lee, J. K., Noh, W. C., & Park, I. C. (2016). Dichloroacetate potentiates tamoxifen-induced cell death in breast cancer cells via downregulation of the epidermal growth factor receptor. *Oncotarget*, *7*(37), 59809-59819.

- Woolbright, B. L., Choudhary, D., Mikhalyuk, A., Trammel, C., Shanmugam, S., Abbott, E., Pilbeam, C. C., Taylor, J. A., & III. (2018). The Role of Pyruvate Dehydrogenase Kinase-4 (PDK4) in Bladder Cancer and Chemoresistance. *Molecular Cancer Therapeutics*, *17*(9), 2004-2012.
- Woolbright, B. L., Rajendran, G., Harris, R. A., & Taylor, J. A. (2019). Metabolic flexibility in cancer: Targeting the pyruvate dehydrogenase kinase:pyruvate dehydrogenase axis. *Molecular Cancer Therapeutics*, *18*(10), 1673-1681.
- Wu, S., Pan, Y., Mao, Y., Chen, Y., & He, Y. (2021). Current progress and mechanisms of bone metastasis in lung cancer: A narrative review. In *Translational Lung Cancer Research*, *10*(1), 439-451.
- Yamao, M., Naoki, H., Kunida, K., Aoki, K., Matsuda, M., & Ishii, S. (2015). Distinct predictive performance of Rac1 and Cdc42 in cell migration. *Scientific Reports*, *5*, 17527. <https://doi.org/10.1038/srep17527>.
- Yang, Zheng, & Tam, K. Y. (2016). Anti-cancer synergy of dichloroacetate and EGFR tyrosine kinase inhibitors in NSCLC cell lines. *European Journal of Pharmacology*, *789*, 458-467.
- Yang, Zuyao, Hackshaw, A., Feng, Q., Fu, X., Zhang, Y., Mao, C., & Tang, J. (2017). Comparison of gefitinib, erlotinib and afatinib in non-small cell lung cancer: A meta-analysis. *International Journal of Cancer*, *140*(12), 2805-2819.
- Yoshida, G. J. (2015). Metabolic reprogramming: The emerging concept and associated therapeutic strategies. In *Journal of Experimental and Clinical Cancer Research*, *34*, 111. <https://doi.org/10.1186/s13046-015-0221-y>.
- Yuan, M., Huang, L. L., Chen, J. H., Wu, J., & Xu, Q. (2019). The emerging treatment landscape of targeted therapy in non-small-cell lung cancer. In *Signal Transduction and Targeted Therapy*, *4*, 61. <https://doi.org/10.1038/s41392-019-0099-9>.
- Zappa, C., & Mousa, S. A. (2016). Non-small cell lung cancer: Current treatment and future advances. *Translational Lung Cancer Research*, *5*(3), 288-300.
- Zhao, H., Mao, J., Yuan, Y., Feng, J., Cheng, H., Fan, G., Zhang, Y., & Li, T. (2019). Sodium dichloroacetate stimulates angiogenesis by improving endothelial precursor cell function in an AKT/GSK-3 $\beta$ /Nrf2 dependent pathway in vascular dementia rats. *Frontiers in Pharmacology*, *10*, 523. <https://doi.org/10.3389/fphar.2019.00523>.
- Zirlik, K., & Duyster, J. (2018). Anti-Angiogenics: Current Situation and Future Perspectives. *Oncology Research and Treatment*, *41*(4), 166-171.
- Zuazo-Gaztelu, I., & Casanovas, O. (2018). Unraveling the role of angiogenesis in cancer ecosystems. In *Frontiers in Oncology*, *8*, 248. <https://doi.org/10.3389/fonc.2018.00248>.

